

A Probabilistic Framework for Lexicon-based Keyword Spotting in Handwritten Text Images

E. Vidal, A.H. Toselli, J. Puigcerver

April 13, 2021

Abstract

Query by String Keyword Spotting (KWS) is here considered as a key technology for indexing large collections of handwritten text images to allow fast textual access to the contents of these collections. Under this perspective, a probabilistic framework for lexicon-based KWS in text images is presented. The presentation aims at providing a tutorial view which helps understanding the relations between classical statements of KWS and the relative challenges entailed by these statements. More specifically, the development of the proposed framework makes it self-evident that word recognition or classification implicitly or explicitly underlies any formulation of KWS. Moreover, it clearly suggests that the same statistical models and training methods successfully used for handwriting text recognition, can advantageously be used also for KWS, even though KWS does not generally require or rely on any kind of previously produced image transcripts. These ideas are developed into a specific, probabilistically sound approach for segmentation-free, lexicon-based, query-by-string KWS. Experiments carried out using this approach are presented, which support the consistency and general interest of the proposed framework. Several datasets, traditionally used for KWS benchmarking are considered, with results significantly better than those previously published for these datasets. In addition, results on two new, larger handwritten text image datasets are reported, showing the great potential of the methods proposed in this paper for indexing and textual search in large collections of handwritten documents.

1 Introduction

Massive quantities of historical manuscripts have been converted into high resolution images in the last decades as a result of digitalization works carried out by archives and libraries world wide. Billions of handwritten text images have been produced through these efforts, and this is only a minuscule part of the amount of handwritten documents which are still waiting to be digitalized. The aim of manuscript digitization is not only to improve preservation, but also to make the handwritten documents easily accessible to interested scholars and general public. However, access to the real wealth of these images, namely, their *textual contents*, remains totally elusive. Consequently, there is a fast growing interest in automated methods which allow the users to search for relevant textual information contained in handwritten text images.

In order to use classical Information Retrieval (IR) methods [40] for plain-text indexing and search, a first step would be to convert the handwritten text images into digital text. But the image collections for which text indexing is highly in demand are so large that the cost of manually transcribing these images is entirely prohibitive, even using crowd-sourcing approaches. An obvious alternative to manual transcription is to rely on automatic Handwritten Text Recognition (HTR) [3, 81, 70]. However, despite the great recent advances in the field [22, 15, 59], fully automatic transcripts of the kind of historical images of interest still lack the accuracy required to enable useful plain-text indexing and search. Another possibility is to use computer-assisted transcription methods [74, 57], but so far these methods can not provide the huge human-effort reductions needed to render semiautomatic transcription of large image collections feasible [71].

HTR accuracy becomes low on real historical handwritten text images for many reasons, including unpredictable, erratic layouts, lines with uneven interline spacing and highly variable skew, etc. In addition, unambiguous reading order of layout elements is often difficult or impossible to determine. Current state of the art HTR systems achieve good transcription results only if perfect layout, line detection and reading order are taken for granted (as it is often the case in published results). Clearly, for moderate sized image collections, many of these problems can often be fixed by simple and inexpensive manual post-processing, but this is completely impracticable when collections of hundreds of thousands, or millions of images are considered.

Interestingly, most or all of these problems disappear or become much less severe if, rather than to achieve accurate word-by-word image transcripts, the goal is to determine how likely is that a given word is or is not written in some indexable image region, such as a text line, an arbitrary text block, or just a full page image. This goal statement places our textual information retrieval problem in the field broadly known as Keyword Spotting (KWS). A comprehensive survey of KWS techniques has recently been published in [20]. Among the works cited in this survey, it is worth noting that many recent developments are inspired in one form or the other in earlier KWS works in the field of automatic speech recognition (ASR), such as [11, 58, 64, 9, 10]. This is also the case of the work presented in this paper.

Generally speaking, KWS aims at determining *locations* on a text image or image collection which are likely to contain instances of the query words, without explicitly transcribing the image(s). One of the earliest statement of KWS for text images, known as “*segmentation-based*” [20], assumes the *locations* to be previously cropped small image regions which contain individual words. Adopting word-sized image regions is a very tempting assumption. But

manual word segmentation is obviously unfeasible for large image collections, and automatic word segmentation can not be reliably carried out, because word separation is often nonexistent and/or notoriously inconsistent in most historical handwritten documents. This is in contrast with “*segmentation-free*” KWS formulations [20], which consider that finding the word locations and determining how likely the corresponding image regions may contain a query word are dual aspects of the same problem.

Many recent works assume an intermediate view of KWS where relatively large image regions (such as lines or paragraphs), which typically contain several words, are considered the search targets where word relevance likelihoods have to be determined. This view, which is often referred to also as (word-)segmentation-free, is called “*line-segmentation-based*” in [20]. It is particularly interesting because it can very adequately support the kind of indexing and search features needed to provide textual access to large collections of handwritten images – and, moreover, automatic image segmentation into these larger regions is generally very much less problematic than individual word segmentation. Most of the developments and results of this paper loosely adhere to this view.

Another traditional taxonomy in KWS distinguishes *Query-by-Example* (QbE) and *Query-by-String* (QbS) formulations, depending on whether query words are specified by means of example-images or just as character strings, respectively [20]. While there are applications for which the QbE scenario can certainly be useful, it is clearly inappropriate for effective indexing and search in large image collections. Therefore, in this paper only the QbS framework is considered.

As we will see, HTR and KWS can advantageously share the same statistical models and training methods. However, it is important to realize that HTR and KWS are fundamentally different problems, even if both may rely on identical probability distributions and models. The HTR decision rule attempts to obtain the best sequence of words (transcript) for a given (line) image region. Therefore the result epitomizes just the *mode of the distribution*; once a transcript has been obtained, the distribution itself can be safely discarded. In contrast, KWS decisions are delayed to the query phase and, for each decision, the *full distribution* can (should!) be used. This obviously explains why proper KWS can always achieve better overall indexing and search results than those provided by naive KWS based on plain HTR transcripts.

An indexing and search system can be evaluated by measuring its *precision* and *recall* performance for a given (large) set of keywords. Precision is high if most of the retrieved results are correct while recall is high if most of the existing correct results are retrieved. In the case of indexed automatic HTR transcripts, precision and recall are fixed numbers, which are obviously closely correlated with the accuracy of the recognized transcripts. In contrast, for a KWS system based on the likelihood that a keyword is written in an image region, arbitrary precision-recall tradeoffs can be obtained by setting a threshold to decide whether the likelihood is high enough or not. We refer to this flexible search and retrieval framework as the “*precision-recall tradeoff model*”. Under this model, it becomes even more clear that proper KWS has the opportunity of achieving better results than naive KWS based on HTR transcripts, as previously discussed.

Some of the developments and results presented in this paper are based on techniques described in [78], or follow research directions outlined in that paper. Contributions of this paper to the state of the art in KWS for handwritten image indexing and search include: First, a sound probabilistic framework is presented which helps understanding the relations between classical statements

of KWS and the relative challenges entailed by these statements. Second, the development of this framework makes it self-evident that word recognition implicitly or explicitly underlies any formulation of KWS, and clearly suggests that the same statistical models and training methods successfully used for HTR can advantageously be used also for KWS. Third, these ideas are developed into a specific, probabilistically sound approach for segmentation-free, lexicon-based, query-by-string KWS. Fourth, experiments carried out using this approach on datasets traditionally used for KWS benchmarking yield results significantly better than those previously published for these datasets. And fifth, KWS results on two new, larger handwritten text image datasets are reported, showing the great potential of the methods proposed in this paper for accurate indexing and textual search in large collections of handwritten documents.

The remaining sections of this paper are as follows: The proposed general framework is introduced in Sec. 2 and developed in the following sections. Sec. 3 introduces the concept of pixel-level word posteriors. While this concept is instructive, the computational costs entailed are exceedingly high. Therefore, in Sec. 4, we develop the idea of computing relevance probabilities for adequate sized image regions and explain how these relevance probabilities can be accurately and efficiently computed when the image regions considered are text line regions. In Sec. 5 we briefly review popular KWS approaches under the proposed statistical framework and discuss our specific proposal. The experimental settings are presented in Sec. 6 and the corresponding results in Sec. 7. Finally Sec. 8 concludes the paper summarizing the work carried out and outlining future avenues of research.

2 A Probabilistic Framework for Word Spotting

In the literature of Key Word Spotting for Text Images, outlined in Sec. 1, two main questions are being considered, regarding a query word v and a certain text image or image region \mathcal{X} :

1. Is the word v written in \mathcal{X} ?
2. What are the locations (if any) of word v within \mathcal{X} ?

The first question is a “simple” yes/no question which, from a probabilistic point of view, must be somehow modeled by a binary random variable. The second question may appear more complex, but it can be reformulated by asking whether each individual location within \mathcal{X} , may contain v or not. Each of these individual questions is again a “simple” yes/no question which can be modeled by a binary random variable, as well. The probabilistic framework presented here deals with these questions.

First, we introduce a random variable X over the set of all image regions considered. A value of this random variable (i.e., an arbitrary image region), will be denoted as \mathcal{X} . At this point we do not need to consider what are the possible sizes and shapes of image regions (a page, a paragraph, a line, etc.) or how they are represented (direct pixel values, or features extracted from these values). Therefore, until we need to be more specific, we will simply use the term “*image*” for a value of X .

Second, we introduce another random variable, Q , over the set of all possible user queries. An arbitrary value of this random variable will be generally denoted as q . To keep the presentation

simple, in this paper we will consider only single-word queries; that is, we focus on conventional word-based QbS KWS, where queries are individual words v from a given vocabulary V , which consists of a set of words we are interested in¹. Nevertheless, the proposed probabilistic framework can properly accommodate arbitrary types of queries: from single words, to regular expressions of characters or words, or even “example image patches”, as in QbE KWS (see, for instance [44, 80]).

Third, a random variable over the set of all possible *locations* is needed. Ideally, one would like to consider a word “*location*” as the set of pixels that make up the image rendering of this word. However, such a fine-grained assumption is not generally feasible, nor it is needed in practice, and the location of a word is often considered to be its “*bounding box*”. Therefore, we define the random variable B over the set of all word-sized bounding-boxes in an image and we will use b to denote a specific word location or bounding box.

Finally, we need the binary random variable that we referred to in the very beginning of this section to model the event that a certain image \mathcal{X} (or a particular location, b within it) contains (or not) a specific query q . It will be named R , after “*relevant*”, in order to follow common notation in the field of IR. This entails a reformulation of the original question as: “is the image \mathcal{X} *relevant* for the query q ?”, considering that \mathcal{X} is relevant for q if one (or more) instance(s) of q are rendered in \mathcal{X} .

Using these random variables, we introduce two probability distributions that will help answer the original questions posed by KWS:

$$P(R = \text{yes} \mid X = \mathcal{X}, Q = q) \tag{1}$$

$$P(R = \text{yes} \mid X = \mathcal{X}, Q = q, B = b) \tag{2}$$

The first distribution is the probability that the image \mathcal{X} is relevant for the query q , while the second is the probability that the location b within \mathcal{X} is relevant for the query q . It is obvious to see that the relevance probabilities defined by Eq. (1) and Eq. (2) can be properly interpreted as the statistical expectation that q is written in \mathcal{X} or in b , respectively.

To simplify notation, in what follows we will write $P(R \dots)$ rather than $P(R = \text{yes} \dots)$, except when the full notation helps avoiding ambiguity and/or enhancing clarity. Similarly, other random variables will be omitted; i.e., we will write $P(a \dots)$ rather than $P(A = a \dots)$.

Simple *marginalization* can be applied to derive the first, more coarsely-grained distribution from the second one:

$$P(R \mid \mathcal{X}, q) = \sum_{b \in B} P(R, b \mid \mathcal{X}, q) = \sum_{b \in B} P(R \mid \mathcal{X}, q, b) P(b \mid \mathcal{X}, q) \tag{3}$$

In the next sections we explain how to compute relevance distributions for given images. We anticipate that most of these developments will rely on the application of the same fundamental marginalization rule used in Eq. (3). We will start in Sec. 3 by introducing the concept of word posteriors computed at the pixel level. While such a representation is conceptually enlightening, its computation is expensive and, moreover, it would require prohibitive amounts of memory and time for keyword indexing and search. Therefore we will argue that keyword search does not

¹A “non-word” token may also be included in V to account for image regions without text.

really need such a fine-grained resolution and, in Sec. 4, we discuss the convenience of computing the required probabilities for whole image regions of adequate size. Then, in Sec. 4.3 and 4.4 we explain how $P(R | \mathcal{X}, q)$ can be derived from pixel-level word posteriors when \mathcal{X} is an adequate image region. Finally, in Sec. 4.5 we explain how these region-level word relevance probabilities can be accurately and efficiently computed when the image regions considered are text line regions.

3 Pixel Level Keyword Search: Image Posteriorgram

We assume that each handwritten page image² has undergone basic preprocessing steps including correction of overall page skew and other simple geometrical distortions [27, 25, 61, 51]. We do *not* need to assume that preprocessing includes any kind of character or word segmentation. Line segmentation is not essentially needed either. Nevertheless, as discussed later on, for effectiveness, efficiency and simplicity, text can be assumed to be organized into distinguishable, roughly horizontal lines.

The *posteriorgram* of a text image \mathcal{X} , is the probability that the query word $q = v \in V$ uniquely and completely appears in a bounding box containing the pixel (i, j) . In mathematical notation:

$$P(Q = v | X = \mathcal{X}, L = (i, j)) \equiv P(v | \mathcal{X}, i, j), \quad 1 \leq i \leq I, 1 \leq j \leq J, v \in V \quad (4)$$

where L is a random variable over the set of locations (pixel coordinates) and I, J are the horizontal and vertical dimensions of \mathcal{X} . $P(v | \mathcal{X}, i, j)$ is a proper probability distribution over the vocabulary V ; that is:

$$\sum_{v \in V} P(v | \mathcal{X}, i, j) = 1, \quad 1 \leq i \leq I, 1 \leq j \leq J \quad (5)$$

A simple way to compute $P(v | \mathcal{X}, i, j)$ is by considering that v may have been written in any possible bounding box b of \mathcal{X} .

$$P(v | \mathcal{X}, i, j) = \sum_{b \in \mathcal{B}(i, j)} P(v, b | \mathcal{X}, i, j) = \sum_{b \in \mathcal{B}(i, j)} P(b | \mathcal{X}, i, j) P(v | \mathcal{X}, b, i, j) \quad (6)$$

where $\mathcal{B}(i, j)$ is the set of all bounding boxes of the image which contain the pixel (i, j) . Fig. 1 illustrates this marginalization process. $P(v | \mathcal{X}, b, i, j)$ is the probability that v is the (unique) word written in the box b (which includes the pixel (i, j)). Therefore it is conditionally independent of (i, j) given b , and Eq (6) simplifies to:

$$P(v | \mathcal{X}, i, j) = \sum_{b \in \mathcal{B}(i, j)} P(b | \mathcal{X}, i, j) P(v | \mathcal{X}, b) \quad (7)$$

Real results of computing the posteriorgram $P(v | \mathcal{X}, i, j)$ in this way for a given image \mathcal{X} and a specific keyword v are shown in Fig. 2.

The distribution $P(b | \mathcal{X}, i, j)$ of Eq. (7) should be interpreted as the probability that some word (not necessarily v) is written in the image region delimited by the bounding box b (which

²The term “page image” is used here for the result of scanning a significant piece of (handwritten) document.

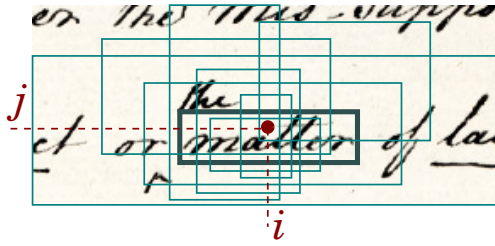


Figure 1: Bounding boxes $b \in \mathcal{B}(i, j)$. For $v = \text{"matter"}$, the thick-line box will provide the highest value of $P(v | \mathcal{X}, b)$, while most of the other boxes will contribute only (very) low values to the sum.

includes the pixel (i, j)). Therefore, this probability should be high for word-shaped and word-sized bounding boxes centered around the pixel (i, j) , like some of those illustrated in Fig. 1. In contrast, it should be low for boxes which are too small, too large, or are too off-center with respect to (i, j) . For simplicity, we could assume that this distribution is uniform for all reasonably sized and shaped boxes around (i, j) and then just replace this distribution with a constant in Eq. (7).

On the other hand, the term $P(v | \mathcal{X}, b)$, is exactly the probability implicitly or explicitly computed by any system capable of recognizing a pre-segmented word image (i.e., a sub-image of \mathcal{X} bounded by b). Actually, such an isolated word recognition task can be formally written as the following classification problem:

$$\hat{v} = \arg \max_{v \in V} P(v | \mathcal{X}, b) \quad (8)$$

In general, any system capable of recognizing pre-segmented word images implicitly or explicitly computes $P(v | \mathcal{X}, b)$ and can thereby be used to obtain the posteriorgram according to Eq. (7).

Obviously, the better the classifier, the better the corresponding posteriorgram estimates. This is illustrated in Fig. 2, which shows two examples of image posteriorgram obtained according to Eq. (7) using two different word image recognizers. In both cases, well trained optical hidden Markov models (HMM) were used to compute $P(v | \mathcal{X}, b) \forall b \in \mathcal{B}(i, j)$. $P_0(v | \mathcal{X}, i, j)$ was obtained directly, using a plain, context-agnostic optical recognizer, and $P_2(v | \mathcal{X}, i, j)$ was produced using a more precise *contextual word recognizer*, additionally based on a well trained bigram. As it can be seen, P_0 values are only good for the two clear instances of “**matter**”, and almost vanish for a third instance, probably because of the faint character “**m**”. Worse still, P_0 values are relatively high for the similar, but wrong word “**matters**”; in fact very much higher than for the third, faint instance of the correct one. In contrast, the contextual recognizer led to high P_2 values for all the three correct instances of “**matter**”, even for the faint one, while the values for the wrong word were very low. Clearly bigrams such as “**It matter**” and “**matter not**” are unlikely, thereby preventing $P_2(v | \mathcal{X}, b)$ to be high for any b around the word “**matters**”. On the other hand, the bigrams “**the matter**” and “**matter of**” are very likely, thereby helping the optical recognizer to boost $P_2(v | \mathcal{X}, b)$ for boxes b around the faint instance of “**matter**”.

Pixel-level posteriorgrams could be directly used for keyword search: Given a threshold $\tau \in [0, 1]$, a word $v \in V$ is spotted in all image positions where $P(v | \mathcal{X}, i, j) > \tau$. Varying τ , adequate *precision–recall* tradeoffs could be achieved.

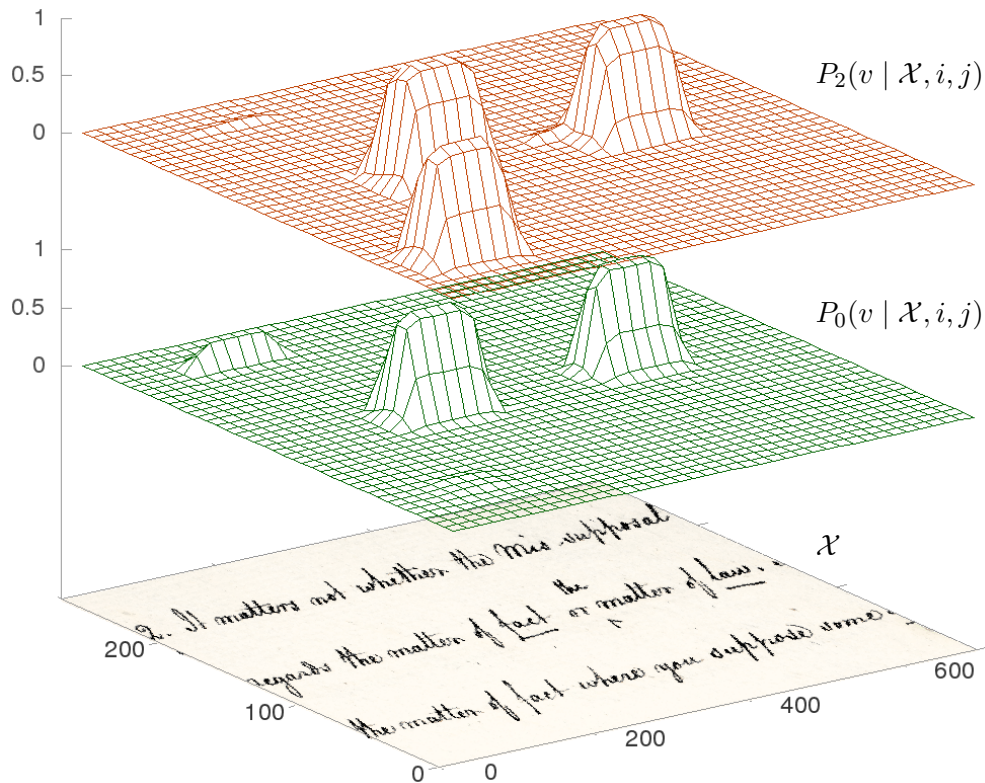


Figure 2: Well trained optical HMM classifiers were used to compute two 2-D posteriorgrams for a text image \mathcal{X} and keyword $v = \text{"matter"}$. P_2 was obtained using a contextual, bigram-based classifier, and provides much better posterior estimates than those of P_0 , computed using a context-agnostic isolated word classifier based on identical optical models.

4 Image-Region Keyword Indexing and Search

Computing the full posteriorgram as in Eq. (7) for all the words of a large vocabulary (as needed for indexing purposes) and all the pixels of each page image of the collection to be indexed entails a formidable amount of computation. Therefore such a direct approach becomes completely prohibitive for the size of handwritten text image collections which are the target of the indexing methods considered in this paper. The same can be said for the exorbitant amount of memory which would be needed to explicitly store all the resulting posterior probabilities. Therefore, rather than working at the *pixel level*, some adequate *image regions*, x , which are smaller than \mathcal{X} and are suitable search targets for users, need be defined to compute the relevance probabilities introduced in Sec. 2. While this problematic is seldom discussed explicitly in the traditional KWS literature, *region proposal* [50] has been the focus of a number of studies in the object recognition community – see e.g. [14], which deals with graphic pattern spotting in historical documents.

In the traditional KWS literature, word-sized regions are often considered. This is reminiscent of segmentation-based KWS approaches which required previously cropped accurate word bounding boxes. However, as discussed in Sec. 1, this is not realistic for large image collections. More importantly, by considering isolated words, the underlying word recognizer can not take advantage of word linguistic context to achieve good spotting precision (as illustrated in Fig. 2).

At the other extreme we may consider whole page images, or relevant *text blocks* thereof, as the search target image regions. While this can be sufficiently adequate for many indexing and search applications, a page may typically contain many instances of the word searched for and, on the other hand, users generally like to get narrower responses to their queries.

A particularly interesting intermediate search target level consists of *line-shaped regions*. Lines are useful targets for indexing and search in practice and, in contrast with word-sized image regions, lines generally provide sufficient linguistic context to allow computing very precise word classification probabilities. Moreover, as will be discussed in Section 5, line region posteriorgrams can be very efficiently computed.

4.1 Image-Region Word Posteriors are not Adequate

A fairly widespread idea in recent works on line-region KWS is to build on whole-region word posterior probabilities, $P(v | x)$. Despite their popularity, it should be pointed out that these word posteriors are *not* directly suitable for region-level keyword search; Instead, they are appropriate to solve the following $|V|$ -class classification problem:

“Given an image region x , find a (*single*) word $v \in V$ which most likely appears in x ”

The associated *Bayes decision rule* [12] is to classify x as:

$$\hat{v} = \arg \max_{v \in V} P(v | x) \quad (9)$$

The intuition behind this classification problem and the corresponding decision rule is unclear: What is the meaning of the (unique) “most likely word” \hat{v} we are looking for? Are we searching for a kind of “most dominant” word within x ? Moreover, $P(v | x)$ sums up to one for all $v \in V$ and therefore the decision rule in Eq. (9) “discriminates” among words in V ; but, for keyword search, each word actually written in x should have high probability and we should rather expect that the sum to be much larger than 1 – in fact it should approach the expected number of different words written in x (cf. Sec. 4.7).

The following example illustrates these inconsistencies according to the probabilistic framework introduced in Sec. 2. Suppose a text image x contains the text “**the cloud is white**”. Then, an *ideal* relevance distribution would be:

$$P(R | v, x) \approx \begin{cases} 1 & v = \text{“the”} \\ 1 & v = \text{“cloud”} \\ 1 & v = \text{“is”} \\ 1 & v = \text{“white”} \\ 0 & \text{otherwise} \end{cases}$$

In contrast, the values of $P(v | x)$ should be much lower for all the four words appearing in x , while the probabilities for other non-relevant words may be significant.

It is worth noting, however, that $P(v | x)$ is perfectly adequate if x is reduced to just the bounding box of each single written word to be searched for. This is in fact the advantage which allows some segmentation-based approaches to KWS to achieve reasonable results – at the expense of requiring previously given accurate word segmentations of the text images.

Assuming for simplicity that the positions (i, j) where the words to be searched for may appear are uniformly distributed, $P(v | x)$ can be readily obtained as a pixel-average of the posteriorgram:

$$P(v | x) = \sum_{ij} P(v, i, j | x) = \sum_{ij} P(i, j | x) P(v | x, i, j) \approx \frac{1}{IJ} \sum_{ij} P(v | x, i, j) \quad (10)$$

where IJ is the number of pixels of x . This approach will be used in Sec. 7, to empirically confirm that using $P(v | x)$ actually leads to poor line-region KWS results.

4.2 Proper Classification Model for Image-Region Keyword Search

Clearly, the classification problem underlying region-level KWS is *not word recognition*. Instead, KWS entails a related but different 2-class classification problem for each word $v \in V$:

Given v , classify each line image x into one of two classes:

- yes : v is (one of the words) written (somewhere) in x
 - not : v does not appear in x
- (11)

As in any binary decision problem, the *cost* of the decision taken can be decomposed in a *loss* matrix, or function:

		Decision	
		No	Yes
Truth	No	λ_{NN}	λ_{NY}
	Yes	λ_{YN}	λ_{YY}

Then, using the posterior probability underlying this classification problem, which is in fact the relevance distribution introduced in Sec. 2, $P(R | x, v)$, the *optimal* decision (i.e. the Bayes, or Minimum Expected Risk, decision) [12], results in answering yes *iff*:

$$P(R | x, v) > \tau = \frac{\lambda_{YN} - \lambda_{NN}}{\lambda_{NY} - \lambda_{YY} + \lambda_{YN} - \lambda_{NN}} \quad (12)$$

Note that in this two-class case, λ reduces to a single threshold τ , which can be adjusted to achieve varying *precision–recall* tradeoffs, as required in KWS. A special case of this decision rule is when making no errors is not penalized (i.e. $\lambda_{NN} = \lambda_{YY} = 0$) and all errors are penalized equally (i.e. $\lambda_{YN} = \lambda_{NY}$). In such special case, the *optimal* threshold reduces to $\tau = 0.5$.

In the following sub-sections we will explain different ways to properly and efficiently compute $P(R | x, v)$.

4.3 Computing Image-Region Relevance Probabilities

Let the correct transcript of an image region x be the sequence of words $w = w_1, w_2, \dots, w_n$, $w_k \in V, 1 \leq k \leq n$, and let us abuse the notation and use $v \in w$ to denote that $\exists k, w_k = v$. The definition of the class yes in Eq. (11) can then be written as:

$$(R = \text{yes}) \equiv (w_1 = v \vee w_2 = v \dots \vee w_n = v) \equiv (v \in w) \quad (13)$$

Of course, if w were known, the relevance probability $P(R | x, v)$ would trivially be 1 if $v \in w$ and 0 otherwise. In practice, no transcripts are available, but an obvious, naive idea is to approximate w with a best transcription hypothesis, $\hat{w}(x)$, produced by a HTR system (see Sec. 4.7):

$$P(R | x, v) \approx \begin{cases} 1 & \text{if } v \in \hat{w}(x) \\ 0 & \text{otherwise} \end{cases} \quad (14)$$

While the simplicity of this idea makes it really enticing (and it has in fact become quite popular), we anticipate that $\hat{w}(x)$ is seldom accurate enough in practice, and this method generally results in poor *precision-recall* performance.

According to [79] and the definition of R in (13), $P(R | x, v)$ can be exactly written as :

$$\begin{aligned} P(R | x, v) &= \sum_{k=1}^n P(w_k = v | x) \\ &\quad - \sum_{l < k} P(w_k = v, w_l = v | x) \\ &\quad + \sum_{m < l < k} P(w_k = v, w_l = v, w_m = v | x) \\ &\quad \dots (-1)^{n-1} P(w_1 = v, \dots, w_n = v | x) \end{aligned} \quad (15)$$

If the image regions are sufficiently small (e.g., line regions), it can reasonably be expected that only one instance of each keyword may appear in each region. In these cases, all the joint probabilities in Eq. (15) vanish and it simplifies to:

$$P(R | x, v) \approx \sum_{1 \leq k \leq n} P_{kvx} \quad (16)$$

where, to simplify notation, P_{kvx} is defined as:

$$P_{kvx} \stackrel{\text{def}}{=} P(w_k = v | x) \quad (17)$$

Note that replacing the sum in Eq. (16) with a *probability average* would result in a deficient distribution and therefore a worse approximation to $P(R | x, v)$. However, a drawback of Eq. (16) is that, in the (generally uncommon) cases where a keyword appears more than once in an image region, $P(R | x, v)$ may become improper since the sum can be greater than one.

Therefore, we propose a simpler approximation to Eq. (15) which, as will be seen later, is better in general and, moreover, it is intuitively appealing (see Fig. (2) and (4) for illustration).

$$P(R | x, v) \approx \max_{1 \leq k \leq n} P_{kvx} \quad (18)$$

A similar approximation has been used as a popular, good heuristic for *confidence estimation* in many works of automatic speech and handwritten text recognition [60, 65], and recently also for keyword indexing and search in [78].

A less simple, but hopefully better approximation to Eq. (15) can be derived by using the naive Bayes approximation to the joint probabilities of Eq. (15):

$$P(R | x, v) \approx \sum_{k=1}^n P_{kvx} - \sum_{l < k} P_{kvx} P_{lvx} + \sum_{m < l < k} P_{kvx} P_{lvx} P_{mvx} \dots (-1)^{n-1} P_{1vx} \dots P_{nvx} \quad (19)$$

It can then be shown by simple induction that Eq.(19) can be efficiently computed by dynamic programming according to the following recurrence relation:

$$P(R | x, v) \approx q(n), \quad \text{where } q(k) = \begin{cases} P_{1vx} & \text{if } k = 1 \\ P_{kvx} + q(k-1)(1 - P_{kvx}) & \text{if } k > 1 \end{cases} \quad (20)$$

4.4 Estimating Image-Region Relevance Probabilities from Posteriorgrams

In proper KWS no transcript of x is available, but $P(w_k = v | x) \equiv P_{kvx}$ can be estimated from the posteriorgram for $k \in \{1, 2, \dots\}$. To this end, we can divide the whole region x , into n (maybe slightly overlapping or disjoint) sub-regions or blocks, $B_1, \dots B_k, \dots B_n$, where a sufficiently high and wide (usually rather flat) local maximum of $P(v | x, i, j)$ is observed in each B_k for some $v \in V$ (see Fig. 2, where n should be around 25 or, more concretely, the uni-dimensional illustration of Fig. 4, where n would be 9 or 10). Then,

$$P_{kvx} \approx \max_{(i,j) \in B_k} P(v | x, i, j) \quad (21)$$

This estimate can be used in any of the approximations (14,16,18,20) of Sec. 4.3. But it becomes particularly simple in Eq. (18):

$$P(R | x, v) \approx \max_{1 \leq k \leq n} \max_{(i,j) \in B_k} P(v | x, i, j) = \max_{i,j} P(v | x, i, j) \quad (22)$$

Note that the number of sub-regions, n , needed to derive Eq. (22), finally becomes irrelevant.

Clearly, the maximization of Eq.(22) can be carried out during the process of computing $P(v | x, i, j)$ itself and this approach does not add any computational cost to that of obtaining the posteriorgram. Moreover, this approach straightforwardly allows us to locate the precise position of the spotted word within a spotted region x , just as the $\arg \max$ of Eq. (22). For instance, if x is the image region of Fig. 2, spotted while searching for the word "**matter**", an instance of this word can be readily located in a sub-region around $(i = 150, j = 110)$, where $P(v | x, i, j)$ is maximum. Of course, the positions of the other two instances of "**matter**" can also be easily obtained from the posteriorgram.

Eq. (22) heavily relies on the simplest approximation to Eq(15). As suggested in the above derivation of Eq(22), other more direct, posteriorgram-based approximations to $P(R | x, v)$ can be derived by actually dividing the image region x , into n sub-regions or blocks, $B_1, \dots B_k, \dots B_n$, by locating adequately large and wide local maxima of $P(v | x, i, j)$. Then, all the other equations (14,16,20) of Sec. 4.3 can be used to also efficiently and perhaps more accurately compute $P(R | x, v)$. The relative empirical performance of all these approximations will be reported in Sec. 7. We anticipate, however, that our best proposal will be Eq. (22), based on Eq. (18).

Techniques similar to those proposed in Section IV of [73] can be used to compute (almost) exact relevance probabilities (using Eq. (28), to be discussed in Sec. 4.7). In contrast to Eq. (22), this approach does not allow to obtain precise locations of the spotted words within the spotted regions and, moreover, it is much more complex and computationally demanding. Nevertheless, for comparison purposes, we have afforded it on one of the small test sets described in Sec. 6.2. The results, summarized in Fig. 3, show that Eq. (22) provides practically exact results for more than 99.5% of the (line) regions and words spotted in this dataset.

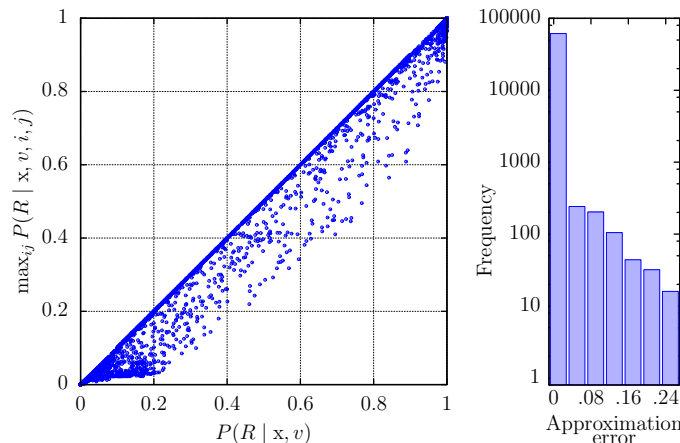


Figure 3: Correlation between exact and approximate relevance probabilities obtained for line regions and words of the Bentham test set. $P(R | x, v)$ is generally well approximated by $\max_{i,j} P(R | x, v, i, j)$ and the approximation error is almost null in more than 99.5% of the regions and words spotted.

From the above discussion, and from the results of Sec. 7, our concluding proposal will be to use Eq. (22). Not only it provides (almost) the best approximation to the ideal relevance probabilities (Eq. (15)), but it also leads to simple implementations and, moreover, it straightforwardly allows to obtain accurate bounding boxes for the spotted words within the spotted image regions.

4.5 Line-Region Keyword indexing and Search

At the beginning of Section 4, line image regions were suggested as particularly adequate search targets for handwritten word indexing and search. More specifically, in connection with the discussion in Sec. 3, the following two main advantages of these regions can be identified:

1. *Line regions* provide sufficiently *rich linguistic context* to allow computing very precise word classification probabilities.
2. Line regions allow for very *efficient computation* of posteriorgrams by smart *choices* of the sets of relevant *marginalization boxes*, $\mathcal{B}(i, j)$ and wise *vertical sub-sampling*.

For a line-shaped region, the relevant sets of *marginalization boxes* needed to compute the posteriorgram according to Eq. (6) can be just defined by *horizontal segmentation*. As will be discussed later, very adequate sets $\mathcal{B}(i, j)$ can be efficiently obtained as a byproduct of using a holistic, context-aware handwritten recognizer on the whole line image region.

On the other hand, in general, *vertical sub-sampling* can just reduce to guessing a proper line height and running a vertical-sliding window of this height with some overlap. However, in many

cases, text line spacing is fairly regular and standard line detection and extraction techniques [37, 36, 38] can yield accurate results. This may lead to computation reductions and potentially increase the precision. The possible lack of robustness of this approach can be easily alleviated by means of *over-segmentation* [7, 33].

In what follows we will assume (as in [30, 66, 19, 17, 28, 85, 78] – see also [20]) line-shaped image regions as our target resolution level for keyword indexing and search. Of course, once a line spot is determined, the exact position(s) of the keyword searched for within the line can be easily obtained as a byproduct (and/or through simple post-processing).

4.6 1-D Posteriorgrams and Line-Region Relevance Probabilities

First, line images are assumed to be submitted to the usual line preprocessing (and maybe feature extraction) steps adopted for line-oriented HTR [3, 70, 54, 59, 22, 15]. This way, each text line image x becomes represented as a sequence, x , of vectors, where each vector \vec{x}_i , $1 \leq i \leq m = |x|$, describes grey-level values (or adequate features thereof) of a narrow vertical box (or “frame”) extracted at uniformly spaced horizontal line positions. The (line-level, 1-D) posteriorgram of x is then (re-)defined as the probability that \vec{x}_i is one of the vectors representing a horizontal segment of x which uniquely contains the word v . It is denoted as:

$$P(v | x, i), \quad 1 \leq i \leq m, \quad v \in V \quad (23)$$

As in the general two-dimensional case, $P(v | x, i)$ can be easily computed by considering that v may appear in any horizontal segment s of x which includes the vector \vec{x}_i :

$$P(v | x, i) = \sum_{s \in \mathcal{S}(i)} P(v, s | x, i) = \sum_{s \in \mathcal{S}(i)} P(s | x, i) P(v | x, s) \quad (24)$$

where $\mathcal{S}(i)$ is the set of reasonably shifted and sized segments which contain the frame i and, as in Eq. (7), $P(s | x, i)$ can be assumed uniform and replaced by an adequate constant. Also in this one-dimensional setting, any system capable of recognizing pre-segmented vector sequences corresponding to word images should explicitly or implicitly rely on computing $P(v | x, s)$ and can thereby be used to obtain the posteriorgram according to Eq. (24).

As discussed previously, an important advantage of line-level processing is that it allows to easily take into account the rich contextual word information provided by words surrounding each query word. In Sec. 5 we will discuss our concrete proposal to efficiently obtain this kind of posteriorgrams using techniques described in [78]. A real example of context-aware line image posteriorgram obtained in this way is shown in Fig. 4.

Finally, Eqs. (20–22) in Sec. 4.3 and Sec. 4.4 can straightforwardly rewritten to obtain line-region relevance probabilities from $P(v | x, i)$. In particular, Eq. (22) becomes:

$$P(R | x, v) \approx \max_i P(v | x, i) \quad (25)$$

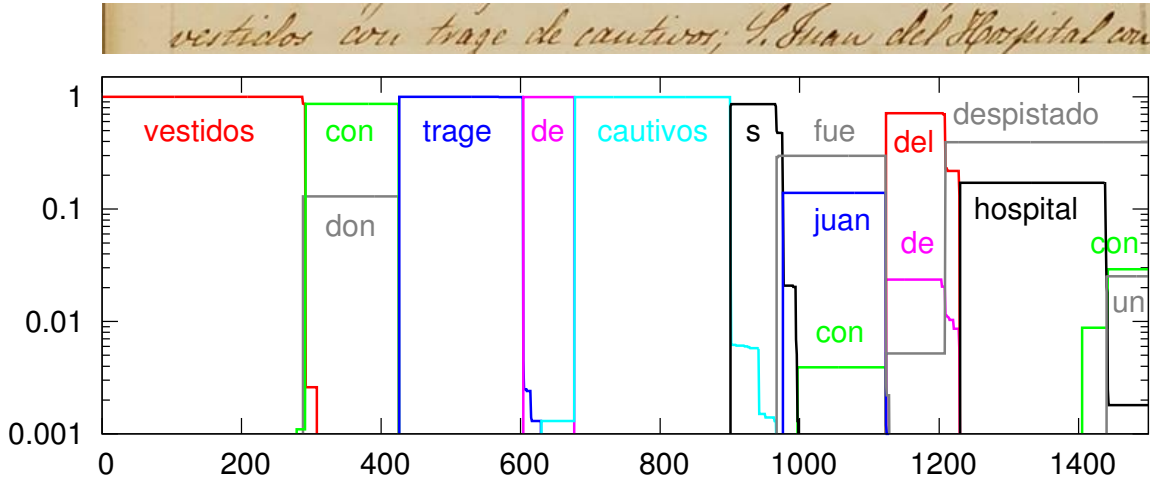


Figure 4: A 1-D posteriorgram obtained with the approach outlined in Sec. 5, using a recognizer based on optical HMMs and a 2-Gram language model.

4.7 Keyword Spotting and Handwritten Text Recognition

Many authors in the field of KWS consider that KWS and HTR are very different problems which should be tackled using distinct approaches or methods. Aiming to shed light on the relationship between these two fields, in this subsection KWS will be re-visited from the HTR point of view. Following the probabilistic framework adopted throughout this paper, we will see that both problems can be properly and advantageously formulated according to identical probability distributions. This firmly suggests that well-established techniques to model and train the probabilistic distributions used in the field of HTR can be advantageously used for KWS, as well. In fact, the most successful handwriting KWS methods (and those in the closely related field of speech KWS, also known as Spoken Term Detection), use in one way or another this relationship.

In Sec. 2, it was pointed out that KWS essentially boils down to answering the question: “is the word v written in the text image region x ?”. Clearly, a direct answer to this question is to check whether v appears in a word sequence w which constitutes the transcript of x . But, since w is unknown, it needs to be considered as the value of a new random variable, W , defined over all the possible transcripts of x . This allows us to obtain the KWS relevance probability by marginalization on W :

$$P(R | x, v) = \sum_w P(R, W = w | x, v) = \sum_w P(R | w, x, v) \cdot P(w | x, v) \quad (26)$$

where W has been omitted as previously done with other random variables and w ranges over the set of all sequences of words in V . Now, since w is given in $P(R | w, x, v)$, it can be written as:

$$P(R | w, x, v) = \begin{cases} 1 & v \in w \\ 0 & \text{otherwise} \end{cases} \quad (27)$$

On the other hand, since image transcripts (w) are independent from user queries (v), the term

$P(w | x, v)$ in Eq. (26) simplifies to $P(w | x)$ and we can write:

$$P(R | x, v) = \sum_{w:v \in w} P(w | x) \quad (28)$$

That is, KWS relevance probabilities can be properly computed on the base of the probability that a sequence of words w is the transcript of the image region x . Interestingly, this is exactly the same distribution used by modern Handwritten Text Recognition systems, which search for a most likely transcript of the given text image region x according to the minimum Bayes error criterion [12]; that is:

$$\hat{w} = \arg \max_w P(w | x) \quad (29)$$

Directly computing KWS relevance probabilities according to Eq. (28) constitutes a complex computational problem. It can be solved by means of a dynamic programming technique similar to the “forward” approach proposed in Section IV of [73]. But, even using this technique, the computational cost is still very high, as the results presented in [73] clearly show. Therefore, in this paper, we will omit these computational details and will only use this approach for comparison purposes.

Nevertheless, adequate approximations can be obtained by extending the naive “1-best” idea based on Eq. (29), discussed in Sec. 4.3. More specifically, the sum in Eq. (28) is restricted to a set of n word sequences for which $P(w | x)$ is largest. This set, often called “ n -best list”, can be obtained as a byproduct of solving the optimization problem of Eq. (29) [26]. If n is large enough, accurate relevance probabilities can be obtained, but computational costs grow exceedingly fast for increasing values of n . While using n -best lists for KWS is promising, more research work is required and we will not elaborate further in this specific direction in the present paper. Instead, as discussed in the previous section, we stick to posteriorgrams efficiently and accurately obtained using word-graph representations of the distribution $P(w | x)$ [78].

5 Proposed Statistical Framework and KWS Approaches

In the framework proposed in Sec. 3, a KWS method is assumed to implicitly or explicitly visit all the image locations (i, j) and all the possible bounding boxes (BB) b containing (i, j) (or adequately selected locations and/or BBs thereof). For each (i, j) and b , an (isolated) word recognizer or word-matching technique of some kind is used to estimate the posterior probability, $P(v | \mathcal{X}, b)$, that a given keyword v is the (only) word written in b . Then Eq. (7) is somehow used to compute the pixel-level posteriorgrams, from which region relevance probabilities are computed as explained in Sec. 4.3 and Sec. 4.4.

A single b encompasses $O(IJ)$ pixels. Thus, estimating $P(v | \mathcal{X}, b)$ for all $v \in V$ can be assumed to be at least $\Omega(NIJ)$, where N is the number of keywords. In general, for each image location there are $O((IJ)^2)$ possible b 's, and the number of locations is $O(IJ)$. Therefore, the overall computational complexity of *directly* computing a posteriorgram in this way, for all the $I \cdot J$ pixels in a full image, is really huge: at least $\Omega(N(IJ)^4)$.

It is then no surprise that the history of development of KWS for text images can be interpreted in terms of how to deal with the different aspects of this exorbitant computational cost.

5.1 Interpretation of Other KWS Methods

According to the framework introduced in this paper, four main aspects can be identified which characterize most (QbS) KWS methods for (handwritten) text images proposed so far.

- How to effectively sample the exceedingly large number of pixel locations of \mathcal{X}
- How to adequately define the set $\mathcal{B}(i, j)$ of marginalization BBs required in Eq. (7)
- How to deal with the summation in Eq. (7)
- How to estimate the word classification posterior $P(v | \mathcal{X}, b)$ for each $b \in \mathcal{B}(i, j)$

We start discussing the first three aspects, which are closely inter-related and together aim to deal with the computational costs which essentially depend on the image size, $I \cdot J$.

All of the early KWS techniques relying on pre-segmented word images [20] circumvented the prohibitive cost of computing Eq. (7) by reducing the summation to just one fixed word-sized image region or “patch”. Moreover, KWS “scores” (proxy for word posteriors) are computed only at the relatively small number, l , of previously given locations of these word patches. This provides a simplistic solution to all the first three aspects discussed above. Obviously, by naively assuming perfect word image detection and segmentation, the computational cost is dramatically reduced down to $O(Nl)$, which clearly explains the mighty popularity of this simplistic idea.

More recent works, such as [55], rely on automatic over-segmentation of the text images to mitigate the impact of word segmentation errors. Such techniques rely on a richer, more realistic sub-sampling and, to some extent, go towards approximating the marginalization in Eq. (6) and (7).

In full segmentation-free KWS methods [20], sub-sampling is generally performed through a *sliding-window* sweep over the image – see, e.g., [24]. However, full pixel-by-pixel sweep is again much too expensive and, in many works, an adequately small number p of *key-points* which define possible parts of the objects of interest (words), are previously located [24, 20]. This way, assuming marginalization is simplistically reduced to just one candidate BB or “patch” – which is usually the case, computational cost can be reduced down to $O(Np)$ where, in general, $p \gg l$.

On the other hand, in KWS approaches which work with (unsegmented) *line* image regions, x , the summation in Eq. (7) becomes uni-dimensional (i.e., Eq. (24)). In many of these approaches the sum in this equation is more or less explicitly approximated only by the dominating addend (which is typically a good approximation – generally much better than relying on a single, given BB). Then, *dynamic programming* techniques are used to avoid repeated computations during a sliding window process over the horizontal positions of x . This is specifically the case of (word-)segmentation-free *dynamic time warping* KWS methods such as [66, 30], as well as all the modern techniques based on HMMs [68, 17, 84] and recurrent neural networks [19].

Nevertheless, obtaining a true full 1-D posteriorgram for each of the L line-regions in \mathcal{X} would still entail a formidable amount of computation. In general, the size of the set of marginalization segments, $S(i)$, is $O(m^2)$ and the the average segment length is $\Theta(m)$, where m is the length

of x , which in turn is $O(I)$. Therefore, even if repeated computations are avoided, the overall asymptotic time complexity is $O(NLI^2)$. Fortunately, in this simpler 1-D case, reasonably good and computationally cheaper approximations can be obtained in a variety of ways. Below we will outline the approach we propose and we have used to obtain the results reported in Sec. 7.

Let us now discuss the last aspect which characterize a KWS; namely how to estimate the word classification posteriors $P(v | \mathcal{X}, b)$. Three main approaches can be identified: HMMs, (Recurrent) Neural Networks (RNN) and distance-based.

The most common use of HMMs is to model a word v as an explicit or implicit concatenation of character HMMs. The combined HMM estimates the likelihood that a word image patch (\mathcal{X}, b) is a rendering of the modeled word; i.e., $P(\mathcal{X}, b | v)$, which is proportional to $P(v | \mathcal{X}, b)$ assuming $P(v)$ and $P(b)$ are uniform. Many popular approaches, such as the “*filler*” or “*garbage*” models [17], fall into this category.

Let us now focus on RNN [19]. For a given word image patch (\mathcal{X}, b) , these networks directly provide a sequence of posterior probabilities $P(c | \mathcal{X}, b, i)$ where c is a character and i is a horizontal position within b . For a keyword v , composed of characters c_1, \dots, c_K , dynamic programming can be used to obtain a best matching path $\Phi(\cdot)$, which assign each position i to one of the K characters of v . Then usual independence assumptions lead to the naive Bayes approximation: $P(v | \mathcal{X}, b) \approx \prod_i P(c_{\Phi(i)} | \mathcal{X}, b, i)$, where i ranges over the horizontal positions of b .

Finally, many early approaches to KWS, notably segmentation-based ones, are *based on distances* between representations of queries and images. It is well known that distances can be used to approximate probability distributions in several ways [12]. If y and z are, respectively, representations of a query word v and an image BB (\mathcal{X}, b) , then a very simple estimator of the classification posterior required in Eq. (7) is: $P(v | \mathcal{X}, b) \approx \phi(y, z) / \sum_u \phi(u, z)$, where $\phi(u, z) = \exp(-d(u, z))$, $d(\cdot, \cdot)$ is the distance, and u ranges over (an adequate set of) query word representations.

Distance-based KWS methods [20] often drop the denominator and use just unnormalized “scores”. While the resulting lack of basic probabilistic properties may not change the *individual* average precision of each query (see Sec. 6.1), unnormalized scores are prone to more or less severely hinder the global average precision for a *set of queries*. This problem may also affect HMM and RNN methods based on heuristically defined relevance probabilities, rather than using a proper approximation to $P(R | x, v)$. This leads some authors (e.g., [17]) to resort to using “*local thresholds*” in their evaluation protocols.

Most distance-based methods are QbE, for which many representation schemes and metrics have been proposed [20], but some recent QbS proposals such as [1] are also distance-based.

5.2 Proposed KWS Approach

To finish this section, we discuss here the specific approach we propose to compute accurate, context-aware line-region posteriorgrams, and the corresponding image region relevance probabilities, in an effective and efficient way. It formally follows the statistical framework developed in previous sections and, as previously mentioned, is based on techniques introduced in [78]. The main idea is to use a *Word Lattice* or *Graph* (WG) [45, 78], obtained as a byproduct of solving

Eq. (29) (see Sec. 4.7) by means of an adequate handwritten text recognizer [57, 78]. A WG of a (line) image-region, x , is a very compact representation of huge amounts of alternative image transcription results, including the probability of each of the (millions of) hypothesized words and the corresponding word segmentation boundaries.

The posteriorgram $P(v | x, i)$ can be obtained from a WG of x following essentially the same arguments as in Eq. (16) and Eq. (24). The basic concept is to consider that, for each position i , the “relevant, reasonably shifted and sized” segments in $\mathcal{S}(i)$ are those given by the word segmentation hypotheses associated with all the WG edges, e , labeled with the word v and such that i is included within the segmentation boundaries specified by departing and ending nodes of e . See [78] for more details about this process. These word boundaries are generally very accurate, not only for the words in the best hypothesis of the WG (called the “1-best” transcript), but also for most of the edges associated with high-probability paths of the WG. Therefore these boundaries and probabilities provide highly informative data to allow very accurately computing Eq. (24).

For a line image-region of length I , the computational cost of obtaining a posteriorgram in this way is in $\Theta(\kappa I)$, where κ is a constant which depends on the size of the WG [78]. According to [78, 75], this cost is generally negligible as compared with the cost of producing the WG itself when using an N -gram based, large vocabulary handwritten text recognizer.

The four aspects which characterize a KWS method are now briefly outlined for the proposed approach: To cope with the exceedingly large number of pixel locations in \mathcal{X} , first the image is sampled vertically by adopting line image regions as discussed in Sec. 4.5, and horizontally according to the segmentation boundaries included in the line image region WGs. Similarly, we let the word segments represented in each WG define the sets of marginalization BBs. With these data, we compute the sum of Eq. (24) (or Eq. (7)) in $\Theta(\kappa I)$ as explained in [78]. Finally, as commented before, the word classification posteriors $P(v | \mathcal{X}, b)$ are directly obtained from the WG edges [78] (probabilities which, in turn, were computed essentially as discussed above for HMMs or RNNs).

Given a posteriorgram obtained in this way, the relevance probabilities needed for keyword indexing are obtained according to Eq. (25), or any of the 1-dimensional versions of Eqs. (20–22). So, once the WGs of the L extracted line image regions are available, the overall computational effort per page image is $O(N \kappa L I)$. More details about these costs, including those of WG generations can be seen in [78, 75].

6 Experimental Framework

To evaluate empirically the KWS performance for the different proposed approaches, in this and the following section will be described the evaluation measures, benchmark datasets, query sets and experimental setup for both RNN and HTR optical modeling and different methods for computing the query relevance probability.

6.1 Evaluation Measures

Let \mathcal{Q} be a set of (word) queries and τ be a relevance threshold. The recall, $\rho(q, \tau)$, and the raw (non-interpolated) precision, $\pi'(q, \tau)$, for a given query $q \in \mathcal{Q}$ are defined as:

$$\rho(q, \tau) = \frac{h(q, \tau)}{r(q)}, \quad \pi'(q, \tau) = \frac{h(q, \tau)}{d(q, \tau)} \quad (30)$$

where $r(q)$ is the number of test image regions which are *relevant* for q (according to the ground truth), $d(q, \tau)$ is the number of regions retrieved or *detected* by the system with relevance threshold τ and $h(q, \tau)$ is the number of detected regions which are actually relevant (also called “hits”).

The interrelated trade-off between recall and precision can be conveniently displayed as the so-called *recall-precision* (R-P) curves, $\pi_q(\rho)$ [13]. Any KWS system should allow users to (more or less explicitly) regulate τ in order to choose the R-P operating point which is most appropriate in each query. Good systems should achieve both high precision and high recall for a wide range of values of τ . A commonly accepted scalar measure which meets this intuition is the area under the R-P curve, $\pi_q(\rho)$, here denoted as $\bar{\pi}_q$ and called (raw) *average precision* [88, 52]. In addition, to consider all the queries in \mathcal{Q} , the (raw) *mean average precision* (mAP, denoted as $\bar{\bar{\pi}}$) is used:

$$\bar{\pi}_q = \int_0^1 \pi_q(\rho) d\rho, \quad \bar{\bar{\pi}} = \frac{1}{|\mathcal{Q}|} \sum_{q \in \mathcal{Q}} \bar{\pi}_q \quad (\text{mAP}) \quad (31)$$

Obviously, the mAP is undefined if $\exists q \in \mathcal{Q}$ for which $\bar{\pi}_q$ is undefined, which happens if $r(q) = 0$, that is, if no test-set image region is relevant for q . On the other hand, Eq. (31) equally weights all the queries, thereby ignoring the different amounts of relevant regions for different queries.

To circumvent both of these issues, a global averaging scheme can be adopted by computing the total number of test image regions which are *relevant* for all $q \in \mathcal{Q}$, the total number of regions *detected* with relevance threshold τ and the total number of *hits*, respectively, as:

$$r = \sum_{q \in \mathcal{Q}} r(q), \quad d(\tau) = \sum_{q \in \mathcal{Q}} d(q, \tau), \quad h(\tau) = \sum_{q \in \mathcal{Q}} h(q, \tau) \quad (32)$$

Then the *overall* recall and raw precision, and the (often preferred) *global average precision*, $\bar{\pi}$, referred to as AP, are defined as:

$$\rho(\tau) = \frac{h(\tau)}{r}, \quad \pi(\tau) = \frac{h(\tau)}{d(\tau)}, \quad \bar{\pi} = \int_0^1 \pi(\rho) d\rho \quad (\text{AP}) \quad (33)$$

Even with this averaging scheme, raw precision can still be ill-defined in some extreme cases and, moreover, raw R-P curves can present an undesired distinctive saw-tooth shape [13]. Both of these issues are avoided by the so-called *interpolated precision*, defined as:

$$\pi'(\rho) = \max_{\rho': \rho' \geq \rho} \pi(\rho') \quad (34)$$

Intuitive arguments in favor of $\pi'(\rho)$, which is often adopted in the literature, are discussed in [40].

The same interpolation scheme can be applied to a single query q , resulting in the interpolated R-P curve $\pi'_q(\rho)$. Then, the *interpolated* versions of mAP and AP are straightforwardly computed using $\pi'_q(\rho)$ and $\pi'(\rho)$, rather than $\pi_q(\rho)$ and $\pi(\rho)$, in Eq. (31) and Eq. (33), respectively.

The use of interpolated precision becomes even more necessary for fair evaluation of KWS results of the naive 1-best KWS approach (see Sec. 4.3, Eq. (14) and Sec. 7), where relevance probabilities are 1 or 0, independent of τ . Therefore, in the raw R-P curve, only one R-P point, (ρ_0, π_0) , is defined and the resulting raw AP would be 0, thereby preventing comparison with other KWS approaches. In contrast, the interpolated precision curve becomes $\pi'(\rho) = \pi_0$ if $0 \leq \rho \leq \rho_0$, $\pi'(\rho) = 0$ otherwise, with a resulting interpolated AP: $\bar{\pi} = \pi_0 \cdot \rho_0$.

6.2 Datasets

The main experiments were conducted on two large handwriting datasets, called PLANTAS and BENTHAM. In addition comparative experiments were carried out on smaller, more usual benchmarking datasets; namely, IAM, George Washington and PARZIVAL. In all the cases, ground-truth line segmentation is available, both for training and testing images, and it is used in the experiments. We leave for future works to experiment with the vertical sub-sampling and over-segmentation ideas discussed in Sec. 4.5. The main features of the datasets used in the experiments are described in the following subsections.

PLANTAS Dataset

The seven volumes of the book “Historia de las plantas” (hereinafter shortened as PLANTAS) were written using a quill-pen by Bernardo de Cienfuegos, one of the most outstanding Spanish botanists in the XVII century. The book was written mainly in Spanish, but a significant number of words and full sentences are in Latin and many other languages. Today, this manuscript has become a source of valuable information for research, specially for those interested in the botanical knowledge of that historical period. The originals of PLANTAS are currently available at the *Biblioteca Nacional de España*, and a digital reproduction of it can be found at the Biblioteca Digital Hispánica³. Examples of page images of this dataset are shown in Fig. 5. In this work, only the first volume of PLANTAS (Mss 3357, with 1 035 pages and around 20 000 handwritten text lines) was considered for experimentation.

Using techniques described in [74, 57], PLANTAS was computer-assisted transcribed into tagged text which concomitantly captured both the *diplomatic* and “*modernized*” transcripts, and also certain *semantic* clues [71]. The diplomatic facet captures, as accurately as possible, all what can be seen in the text image (abbreviations, underlined and crossed-out text, interline inserted text, etc.). The modernized component provides abbreviation expansions, normalized capitalization and punctuation, etc. The semantic tags, finally, describe the language of each non-Spanish word and some word functions such as catch-words and hyphenation. In order to improve the computer-assisted experience and effectiveness, tagged transcripts were used as such (tags and dual text included) to increasingly train the language models used for interactive transcription [71]. As

³<http://bdh-rd.bne.es/viewer.vm?id=0000140162>

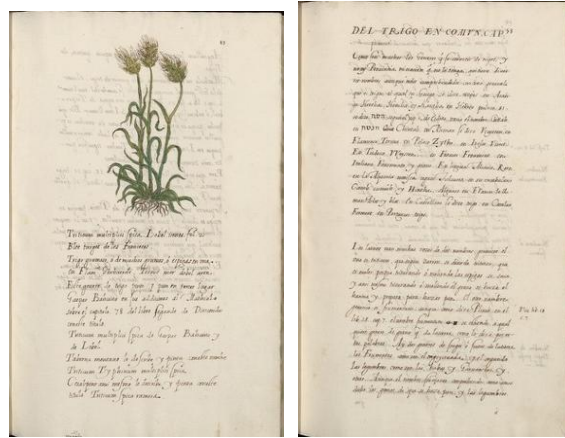


Figure 5: Examples of pages from the first volume of PLANTAS.

discussed later on, the language model used for the experiments presented in this paper was also trained with the fully tagged transcripts of the training images. But only tag-free, *diplomatic* transcripts were employed to obtain the KWS results reported in this paper. See details in Sec. 6.4.

Table 1 shows experimental partitions and general statistics of the PLANTAS tagged dataset. Glossaries, indices, blank page images and images containing only drawings are ignored in the “Image” data. The rows “Running tokens” and “Running OOV” show the total number of tagged words and the percentage of Out-Of-Vocabulary (OOV) tokens, respectively. The OOV tokens in the Validation column correspond to tokens which do not appear as identically tagged words in the training set, while those in the Test column are tokens that do not appear in the training or in the validation sets. Rows labeled “Text” contain data of the training partition which additionally includes extra text, aimed at enhancing language model training, extracted from the glossaries and indices of the excluded page images. Rows labeled “Diplomatic” show the corresponding partitions and statistics of diplomatic reference transcripts used in the KWS experiments reported in this paper. The running words (and lexicon) include the extra diplomatic text from glossaries and indices. Note that, in contrast with the other datasets discussed below, in this part of Table 1 the text is assumed to be *tokenized*; that is punctuation marks are separated and considered as “words”. In addition, validation and test *word error rate* (WER), obtained by a RNN-based HTR system using the same optical and language models as for KWS (see Sec. 6.4), is reported.

The relative sizes of partitions were decided taking into account the experience acquired during the assisted transcription process which was followed to create the dataset ground-truth. More details about this process and the resulting dataset appear in [71].

BENTHAM Dataset

The whole set contains more than 80 000 images of manuscripts written by the renowned English philosopher and reformer Jeremy Bentham (1748-1832) and his secretarial staff [8]. It includes texts about legal reform, punishment, the constitution, religion, and his famous “*panopticon*” prison paradigm.

From the Bentham data currently available, only a relatively small and simple set of 433 page images, written by an unknown number of different writers, is used in this work (see examples in

Table 1: The PLANTAS tagged dataset. Rows labeled “Text” correspond to the training image transcripts plus extra text extracted from glossaries and indices, used to train the language model.

	Number of:	Training	Validation	Test	Total
Image	Pages	224	40	607	871
	Lines	6 788	955	11 801	19 544
	Running tokens	67 912	9 753	117 029	194 694
	Token set size	10 861	2 198	14 018	20 834
	Character set size	76	76	76	76
Text	Running tokens	70 201	9 753	117 029	196 983
	Token set size	11 890	2 198	14 018	21 417
	Running OOV (%)	–	8.95	11.68	–
Diplomatic	Running words	70 201	9 753	117 026	196 980
	Lexicon size	11 045	2 126	13 124	19 693
	Running OOV (%)	–	8.40	10.81	–
	WER (%)	–	15.62	19.61	–

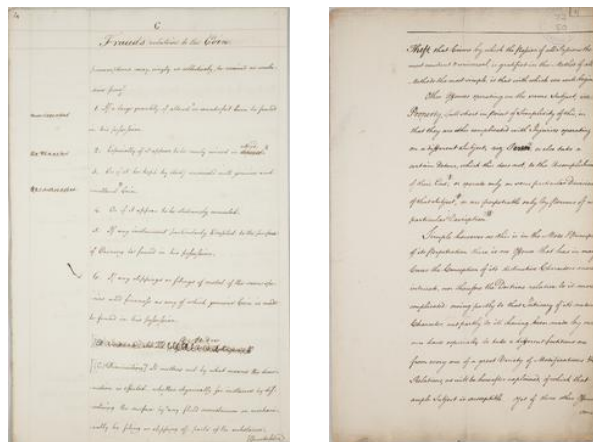


Figure 6: Examples of BENTHAM page images.

Fig. 6). It is exactly the same dataset used in the ICFHR-2014 HTRtS competition⁴ of handwritten text recognition [2]. These pages contain 11 473 lines with nearly 110 000 running words and a vocabulary of more than 9 500 different words. The last column in Table 2 summarizes the basic statistics of these pages. It should be noted that these statistics correspond to *not tokenized* text; that is, each non-blank sequence of characters is assumed to be a “word”, even though it may often correspond to a real word plus a punctuation mark. The dataset was divided into three subsets for training, validation and test. Unlike PLANTAS, which is a single-writer manuscript, BENTHAM was written by many hands, with a large variability in their handwriting styles. Therefore it requires much more training samples to adequately train writer-independent character models. Table 2 shows details of these partitions.

Table 2: The Bentham dataset, used in the ICFHR-2014 HTRtS competition [2].

Number of:	Training	Validation	Test	Total
Pages	350	50	33	433
Lines	9 198	1 415	860	11 473
Running words	86 075	12 962	7 868	106 905
Lexicon size	8 658	2 709	1 946	9 716
Character set size	86	86	86	86
Running OOV(%)	–	6.61	5.30	–
WER(%)	–	13.17	19.76	–

Finally, validation and test WER, obtained by a RNN-based HTR system using the same optical and language models as for KWS (see Sec. 6.4), are also reported in this table. For more details about this dataset refer to [2].

IAM, George Washington and Parzival datasets

IAM is a publicly available, well known modern English handwritten text corpus, compiled by the FKI-IAM Research Group on the base of the Lancaster-Oslo/Bergen Corpus (LOB). The last released version (3.0) is composed of 1 539 scanned text pages, handwritten by 657 different writers and partitioned into writer-independent training, validation and test sets. The line segmentation provided with the corpus [42] is used here. Statistics of the IAM dataset appear in Table 3. In this case for this dataset, the “text” information refers to three external text corpora (LOB, Brown, and Wellington, collectively called “LBW”) which were employed for compiling the lexicon and for training the IAM language model [4].

PARZIVAL (PAR) is a database containing 45 digital images of a medieval manuscript from the 13th century written down in Middle High German language [18]. Although several writers have contributed to the manuscript, all the writing styles found in the data set are very similar. Table 4 presents also information about the employed partition definition and statistics of this data set.

GEORGE WASHINGTON (GW) is a database which includes 20 pages of letters [34] written by George Washington and his associates in the year 1 755. These 20 relatively clean pages, which

⁴www.transcriptorium.eu/~htrcontest/contestICFHR2014/public_html/HTRtS2014

exhibit a very similar writing style, have been selected from a larger collection of images. Because of the small size of the data set, four-fold cross validation has been adopted for experimental evaluation. Therefore, Table 4 includes rounded mean values over all cross validation sets.

Following the standard presentation of these benchmark corpora, as in the case of BENTHAM, all the data in Tables 3 and 4, correspond to *not tokenized* text.

Table 3: The IAM dataset and the corresponding partition. The IAM Running words, Lexicon and OOV (out of vocabulary) figures labeled “Text” correspond to the external text corpora (LBW) used to train the language model.

	Number of:	Training	Validation	Test	Total
Image	Lines	6 161	920	929	8 010
	Running words	53 765	8 599	8 315	70 679
	Lexicon Size	7 771	2 450	2 492	9 749
	Character set size	72	69	65	81
Text	Running words	3 128 155	8 599	8 315	3 145 069
	Lexicon size	19 892	2 450	2 492	20 773
	Running OOV(%)	–	6.12	6.27	–
WER (%)		–	14.22	16.05	–

Table 4: Basic statistics and partition details of the PAR and CW corpora.

Number of:	PAR				GW			
	Training	Valid.	Test	Total	Training	Valid.	Test	Total
Lines	2 237	912	1 328	4 477	328	164	164	656
Running words	14 042	5 671	8 407	28 120	2 447	1 224	1 224	4 894
Lexicon size	3 221	1 753	2 305	4 936	899	539	539	1 471
Character set size	90	80	82	96	79	72	72	83
Running OOV(%)	–	14.58	12.40	–	–	29.26	24.62	–
WER(%)	–	22.08	18.44	–	–	4.27	29.93	–

6.3 Query Sets

Several criteria can be assumed to select the keywords to be used in KWS assessment experiments. Clearly, any given KWS system may perform better or worse depending on the query words it is tested with and how these words are distributed in the test set. Of course, the larger the set of keywords, the more reliable the empirical results. Moreover, since our approach is aimed at indexing applications, testing with a large set of keywords is mandatory.

In this work, taking into account these observations, the adopted criterion for selecting queries for each dataset is to take all the words that appear in their corresponding training partitions. This is exactly true for BENTHAM, PAR and GW datasets, being for this latter selected iteratively

for each training partition of the 4-fold cross-validation (Table 5 shows the query set average size on the 4 cross-validation). Following [19], the line image training lexicon (the one labeled with “image” in Table 3) excluding punctuation marks and *stop words* was used as query set for IAM dataset. Finally, the query set for PLANTAS was extracted from the extended diplomatic lexicon reported in Table 1, by previously filtering out 113 words containing numbers.

It is important to remark that, according to this criterion, there will be many keywords which do not actually appear in any of the test images. We say that these keywords are *non-relevant*, while the remaining ones are *relevant*. Trying to spot non-relevant words is challenging, since other relevant similar words may be erroneously spotted, which may lead to important precision degradations. AP can very aptly used to measure KWS performance for mixed relevant/non-relevant query sets, but mAP is completely inadequate because it can only be computed for relevant words (cf. Sec. 6.1). Table 5 shows the sizes of the query sets used in the five datasets considered.

Table 5: Sizes of the query sets selected for PLANTAS, BENTHAM, IAM, PAR and GW. The amounts of query words for which there is at least one relevant test image are also reported.

Dataset	Keywords	Relevant
PLANTAS	10 932	4 888
BENTHAM	8 658	1 487
IAM	3 421	1 098
PAR	3 221	1 218
GW	899	234

6.4 Experimental Setup

Following the probabilistic KWS framework proposed in this paper, experiments have been carried out to assess the capabilities of specific approaches derived from this framework. These approaches require statistical optical character models and language models which must be trained from the available training images and transcripts. For language modeling we have just adopted the simple and time-honored state-of-the-art N -gram approach [26]. But, for optical modeling, two alternative approaches have been considered: HMMs, which is a well understood, proper statistical approach and RNNs, which are recently showing superb performance in HTR. Both methods have been used in the main (PLANTAS and BENTHAM) experiments, while only RNNs have been used in the comparative experiments with IAM, PARZIVAL and GW.

In general, a similar system architecture is used in all the experiments. However, depending on the dataset and the optical modelling (HMM or RNN) adopted, some details of image pre-processing and feature extraction are different. The general architecture and these details are discussed the coming subsections.

HMM Optical Modeling

For HMM optical modelling, line images were preprocessed for slant, slope and size normalization [70, 56] and then represented as sequences of feature vectors. Feature extraction (for PLAN-

TAS and BENTHAM) was based on geometric moments normalization [31]. A left-to-right HMM topology was used for each character, with the number of states and gaussian densities per state set up taking into account character widths and other general dataset features. Final values of these two meta-parameters were optimized on the validation partition of each corpus. More details about these and other meta-parameter settings for each corpus are given in [77, 41]. HMM training was carried out using *embedded Baum Welch* algorithm [26] using all the training line images and their corresponding transcripts.

Regarding PLANTAS dataset, note that HMM training (and also RNN training in the next section) was carried out using the tokenized diplomatic transcripts, whose basic statistics are presented in Tab. 1.

RNN Optical Modeling

Following the recent success of recurrent neural networks (RNN), in the HTR and KWS fields, RNN optical modelling was adopted, in addition to HMMs, to assess the impact of using different probabilistic models on the proposed KWS framework.

The network is composed of a sequence of four *convolution blocks* aimed to extract meaningful features for the handwritten modeling. Each of these blocks contains a 2D convolutions layer [35] (the number of features extracted in each block is, respectively, 16, 16, 32 and 32), a batch normalization layer, a *LeakyReLU* [39] layer as a non-linear activation function and, finally a 2×2 *max pooling* operation is performed (only in the first three layers), in order to reduce the resolution of the images. The “image” (representation of the extracted features) which results after these convolution blocks, is processed column-wise by a stack of three *bidirectional long short-term memory* (BLSTM) recurrent layers [62, 23]. Finally, each column is linearly transformed to have as many features as characters are in the particular dataset, plus an additional symbol used by CTC. A *softmax* transformation is used to interpret the outputs of the neural network as posterior probabilities. Dropout is used to reduce overfitting in between the BLSTM layers and before the final linear layer output. A general overview of the architecture is depicted in Figure 7.

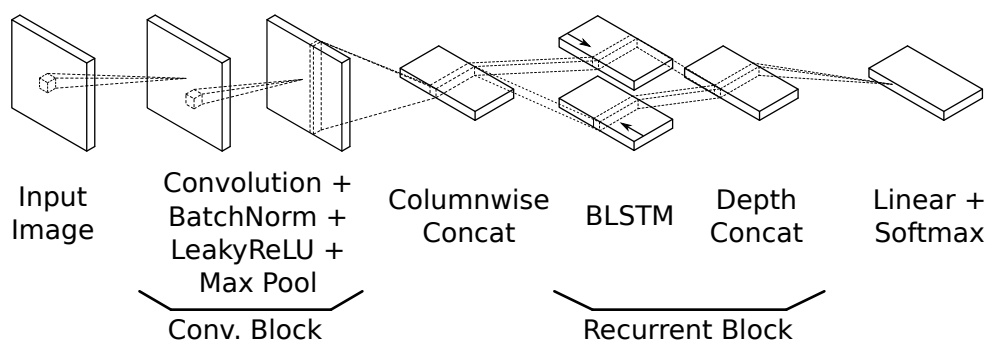


Figure 7: Overview of the neural network architecture used in this work.

Training is performed using the connectionist temporal classification (CTC) algorithm [21], in order to maximize the (log)probability of the training transcripts, given the corresponding images. The parameters of the model are updated using *RmsProp* [69], with a fixed learning rate of 0.0005.

The same architecture and training procedure were used in all the datasets, except IAM, where slightly different hyperparameters were used. In this case, we used the models trained in [48], which have been made public⁵, and have shown an excellent performance in HTR tasks [48].

Finally, in order to combine the output of the neural network with N -gram language models, the posterior probabilities are transformed into pseudo-likelihoods, using the following equation:

$$p(\mathbf{x}_t | l_t) = \frac{P(l_t | \mathbf{x}_t) \cdot p(\mathbf{x}_t)}{P(l_t)} \approx \frac{P(l_t | \mathbf{x}_t)}{P(l_t)^\gamma} \quad (35)$$

where $P(l_t | \mathbf{x}_t)$ is the output of the neural network at column t , $P(l_t)$ was estimated by forced alignment on the training data, and the scaling parameter was fixed to $\gamma = 0.2$ for all datasets.

Lexicon and Language Modeling

For each data set, a lexicon was extracted from the corresponding training partition. For the benchmarking datasets, the standard tokenization for each dataset was adopted. The lexicon of BENTHAM was extracted through a specific, rather straightforwardly improved tokenization scheme, described in detail in [77]. The lexicon of PLANTAS was similarly extracted from the training diplomatic transcripts. For each corpus, except PLANTAS, a 2-gram language model was straightforwardly trained from the corresponding training text, using Kneser-Ney back-off smoothing [29]. For PLANTAS, a 2-gram language model was trained from the raw tagged training text, as discussed in Sec. 6.2. Then tags and modernized word versions were removed, from the resulting model, thereby leaving a diplomatic-only language model for its use in KWS. Viterbi decoding meta-parameters associated with each N -gram language model (*grammar scale factor* and *word insertion penalty*) were tuned to optimize the WER on the corresponding validation set.

Line Image Word-Graphs

The KWS approaches used in the experiments rely on line image WGs, either to compute posteriorgrams, as discussed in Sec. 5, or just to straightforwardly obtain 1-best image transcription hypotheses. WGs are obtained using previously trained optical and language models. For HMM optical models, the procedure is a well-known variation of standard Viterbi decoding, as discussed in detail in [78]. In the case of RNN, Eq. (35) is used to convert the RNN output character posterior probabilities into pseudo-likelihoods, which are then considered as emission probabilities of (typically single-state) character HMMs (see details in [5]). Using these simplified HMMs, the standard HMM approach is followed both to combine character likelihoods and language model probabilities and to obtain the WGs as a byproduct of Viterbi decoding (see [46, 47]).

As discussed in [78, 75], the computational cost of obtaining a WG grows very fast with the WG size. Following [75], in our experiments, WG sizes were controlled by specifying the maximum node input degree [86] and/or by applying *beam-search pruning* during the HTR decoding process. In addition, explicit WG pruning [87] was applied to WG derived from HMM optical models. These WGs were generally (much) larger than those derived from RNN optical models.

⁵<https://github.com/jpuigcerver/Laia>

Therefore, HMM WGs were explicitly pruned down to sizes which, on the average, were similar to those of RNN WGs (see Table 7).

Once WGs had been obtained, they were normalized as discussed in [78]). A normalization parameter (called “logarithm base factor” in [78]) is used in this step to empirically tune the posterior probability calibration [43]. As with the other meta-parameters, this factor was tuned for each optical modelling approach on the validation partition of each corpora.

Posteriorgrams and Line-Region Relevance Probabilities

From the normalized WGs the 1-D posteriorgrams (frame-level word posterior probabilities, $P(v | x, i)$), were obtained as explained in Sec. 4.6.

Finally, line-level word confidence scores, $P(R | x, v)$, were calculated as explained in Sec. 4.3 and 4.4. In particular, Eq. (22) (or, more specifically, its 1-D version, Eq. (25)) is used in all the experiments, while other approaches are tested only in Sec. 7.1.

In two of these approaches, namely those given by Eqs. (16) and (19), a threshold parameter is employed to find significant local maxima on the 1-D posteriorgram. A local maximum is considered as such when the difference $P(v | x, i) - P(v | x, i - 1)$ (proportional to the tangent) becomes negative, surpassing in absolute value a given threshold. As with the other meta-parameters, this threshold value is also optimized using validation partitions.

7 Results

In this section we first use the BENTHAM dataset to empirically explore the relative performance of the proposed approximations to compute keyword relevance probabilities. Then we report final KWS evaluation results for one specific approximation on the five datasets before introduced.

7.1 Testing different Approximations to the Relevance Probability

A first series of experiments were conducted on the BENTHAM dataset, using RNN optical modelling, in order to empirically assess and compare the different approximations for computing the relevance probability $P(R | x, v)$ proposed in Secs. 4.3 and 4.4. Table 6 reports the KWS (interpolated precision) AP performance achieved by these approximations. These approximations range from the roughest one (Eq. (10)), using the $P(v | x)$, to the potentially most accurate, but also much more computationally expensive approximation, given by Eq. (28).

The differences between some of these results are very small and it is unclear whether small superiorities may be due to a better approximation accuracies, or just to differences caused by the presence of non-relevant keywords included in the query set (see Table 5). To help better understanding these small differences, the same experiments were carried out with a smaller query set restricted to just the 1 487 relevant keywords of BENTHAM). For this smaller subset the mAP can be also computed; so, Table 6 also reports the mAP for this subset. These results are denoted as AP_r and mAP_r . In the case of Eq. (19), the parameter used to obtain AP and AP_r was optimized

Table 6: BENTHAM AP for different approximations to the relevance probability $P(R | x, v)$, using RNN optical models. P_{kvx} denotes $\max_{(i,j) \in B_k} P(v | x, i, j)$ (see Eq. (21) in Sec. 4.4). AP_r and mAP_r are reported for the reduced query set of 1 487 relevant queries (see Table 5).

Alternative approximations to $P(R x, v)$	AP	AP_r	mAP_r
Eq. (10): $P(v x)$	0.78165	0.88407	0.94208
Eq. (14): 1 if $v \in \hat{w}$ (1-best transcript); and 0 otherwise	0.76297	0.82063	0.92365
Eq. (16): $\sum_{1 \leq k \leq n} P_{kvx}$	0.87898	0.91767	0.95438
Eq. (18) or (22): $\max_{1 \leq k \leq n} P_{kvx} = \max_{i,j} P(v x, i, j)$	0.91423	0.95155	0.95495
Eq. (19): $\sum_{k=1}^n P_{kvx} - \sum_{l < k} P_{kvx} P_{lvx} + \dots (-1)^{n-1} P_{1vx} \dots P_{nvx}$	†0.91441 0.91289	0.94888 ‡0.95000	0.95445 0.95511
Eq. (28): by using forward algorithm on line-region WGs [73]	0.91297	0.95023	0.95513

on the BENTHAM validation set, using respectively the whole query set (†) and the relevant query subset (‡). As commented in Sec. 6.1, here we also report mAP_r figure only for the relevant query subset.

AP (and mAP) results for approximations given by Eqs. (22), (19) and (28) are practically identical, but the first two are simpler and much less computationally demanding. The computation needed for Eq. (28) is very similar to that of the forward algorithm proposed in Section IV of [73], where the very high cost of that algorithm was empirically studied. The results achieved with the other approaches (Eqs. (10), (14) and (16)) are significantly worse, the naive 1-best KWS technique providing the worst KWS performance.

To summarize, among the approaches considered, Eq. (22) is as good as the best ones, and also the fastest and simplest one. And, also interestingly, it does not have any meta-parameter which needs to be tuned. In what follows, all the results will be reported only for this approach.

7.2 Comparing the Impact of Using HMM or RNN Optical Models

Using only Eq. (22) (or its 1-D version, Eq. (25)), the second series of experiments were devoted to study how different optical modelling choices (HMM and RNN), adopted to compute the posteriorgrams, affect the KWS performance. In addition to the BENTHAM dataset, the other large dataset presented in Sec. 6.2 (PLANTAS) is considered. Table 7 shows the results of this study.

For completeness, results obtained with the naive 1-best KWS approach (Eq. (14)) are also given. For HMMs, results using both original and explicitly pruned WGs are reported. As discussed in Sec. 6.4, this pruning produces WGs of similar average size as that of WGs obtained with RNN optical models. Rather than showing the specific sizes of the WGs (which are meaningless and can be safely discarded once the relevance probabilities are computed), the average number of the spotting alternatives produced for each line region (“Spots/Line”) are reported. For indexing applications, the overall memory requirements are proportional to this “spotting density”. As observed in Tab 7, the AP performance for the explicitly pruned WGs is not significantly de-

Table 7: KWS performance for PLANTAS and BENTHAM using the two optical modelling approaches: HMM and RNN.

Dataset	Optical models	AP	#Spots/Line
PLANTAS	HMMs 1-best	0.722	9.7
	HMMs	0.912	311.9
	HMMs (pruned-WGs)	0.909	128.2
	RNN	0.924	133.9
	RNN 1-best	0.794	9.7
BENTHAM	HMMs 1-best	0.740	8.9
	HMMs	0.910	335.8
	HMMs (pruned-WGs)	0.907	71.2
	RNN	0.914	72.2
	RNN 1-best	0.763	8.4

graded.

Recall – interpolated-Precision (R-P) curves for PLANTAS and BENTHAM obtained using both HMM and RNN optical modelling are plotted in Fig. 8.

According to the results in this section, only small KWS performance differences are observed depending on the choice of HMM or RNN for optical modelling. This applies to both PLANTAS and BENTHAM, both of which are fairly large handwritten corpora and entail important differences between them in many handwriting processing aspects. While RNNs are generally known to be better than HMMs for character optical modeling, the present results suggest that this superiority mainly affects to the mode of the modeled distributions – thereby generally leading to better character error rate results. However, when, as in KWS, the whole distribution is brought into play, the superiority becomes less obvious.

These observations are in line with those of [77], where the transcription performance of both the HMM- and RNN-based HTR systems were also similar, mainly due to the good feature extraction employed for the HMM modelling approach.

7.3 Experiments with Common Benchmarking Data Sets

Additional KWS experiments were carried out with three well established benchmark datasets (see Sec. 6.2): IAM, PARZIVAL (PAR) and GEORGE WASHINGTON (GW). The R-P curves and AP values obtained for these datasets, using RNN optical modelling and relevance probability approximation given by Eq. (18), are presented in Fig. 9.

To place our results in comparison with previously published work, Table 8 presents (word) segmentation-free, query-by-string KWS results obtained by other authors on the same three datasets. The following approaches have been considered: our previous work on lexicon-based HMM KWS [78], bayesian logistic regression classifier (BLRC) [32], character-lattice-based KWS (CL-

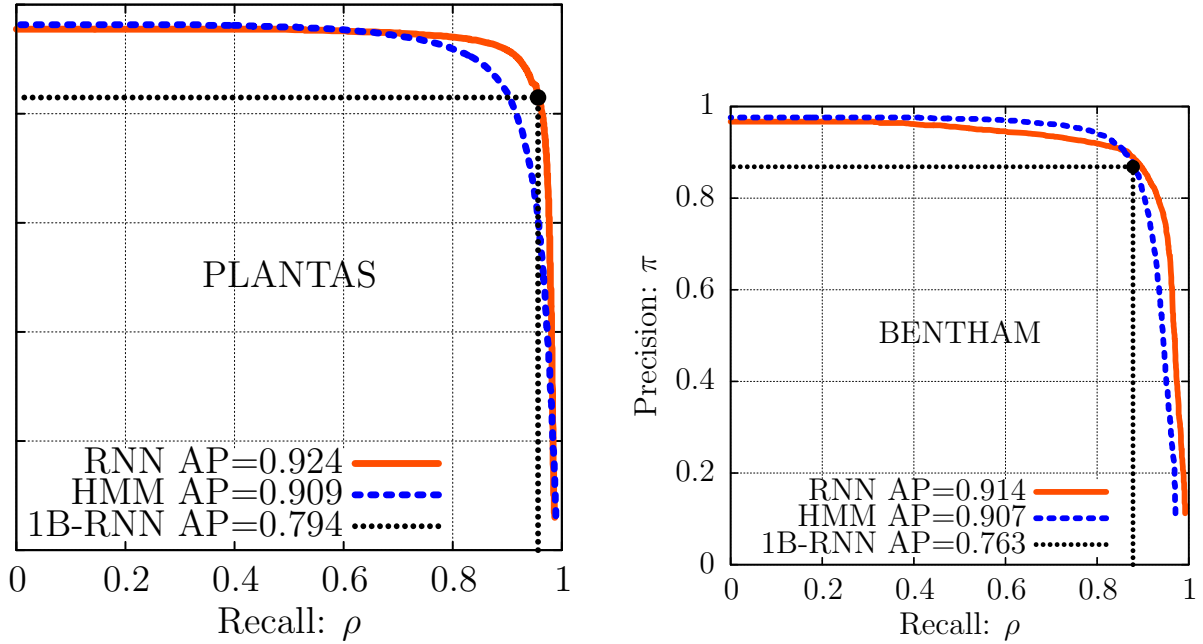


Figure 8: Interpolated R-P curves for PLANTAS and BENTHAM, using optical modelling based on HMMs and RNN. The (degenerate) curves for naive 1-best KWS are also shown

based) [76, 73], dynamic time warping (DTW) [83, 82, 19, 17], bipartite graph matching without rejection (BP) and with fast rejection (BP-FR) [63], bidirectional long-short term memory (BLSTM) [19], convolutional deep belief network (CDBN) [83], local gradient histogram features (LGHF) [82, 53], HMM-filler with background modelling (Filler-B) [85] and histogram of gradients (HOG) [82, 67]. The references with two cites like [82, 53] and [82, 67] indicate that the methods originally presented in [53] and [67] have been applied to obtain comparative results under the experimental setup described in [82]. The pyramidal histogram of characters (PHOC) KWS approach presented in [1] is *not* included because it is *segmentation-based* [20]⁶.

It should be noted that the experimental setups adopted in some of these works may vary significantly with respect to the setup adopted in this work. In particular, in the entries marked with †, KWS performance was obtained using a query set selected from the test partition. Also, in some cases it is not completely clear whether the results are provided in terms of AP or mAP. Therefore, the results of Table 8 can only be considered loosely comparable.

Notwithstanding the slight differences, we conclude that the superiority of the methods proposed in this work can be acknowledged.

8 Conclusions and Outlook

A probabilistic framework for query-by-string, (word-)segmentation-free, lexicon-based KWS, aimed at indexing the textual contents of large collections of handwritten text images, has been

⁶In [1] PHOC results are misleadingly compared with, and considered superior to other state-of-the-art *segmentation-free* methods such as BLSTM [19]

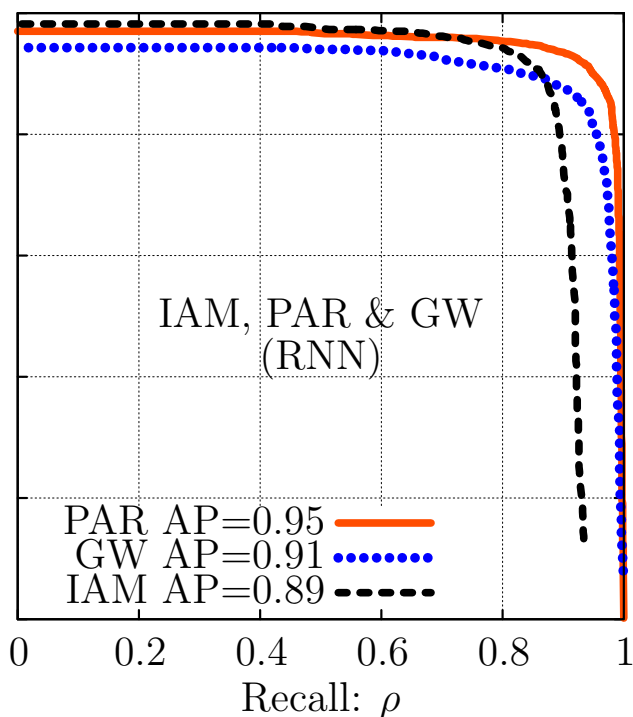


Figure 9: Interpolated R-P curves for the IAM, PAR and GW datasets, using RNN optical modelling and the relevance probability approximation given by Eq. (18).

Table 8: AP results achieved by several line-region KWS approaches on IAM, PAR and GW, with varied empirical setups which may be loosely compared with ours. Values marked with † were obtained using a different query set. The three best results for each dataset are marked in boldface.

Ref.	Approach	IAM	PAR	GW
[82, 53]	LGHF-HMM	0.05 †	0.25 †	0.33 †
[63]	BP-FR	—	0.58 †	0.56 †
	BP	—	0.61 †	0.55 †
[83]	CDBN-DTW	—	0.59 †	0.56 †
[32]	BLRC	0.49 †	—	—
[16]	Classic Filler-HMM	0.48 †	—	0.72 †
	2-gram Filler-HMM	0.55 †	—	0.74 †
[17]	DTW	—	0.39 †	0.44 †
	Classic Filler-HMM	—	0.86 †	0.62 †
[82]	CDBN-DTW	0.01 †	0.73 †	0.57 †
	CDBN-HMM	0.65 †	0.92 †	0.71 †
[82, 67]	HOG-HMM	0.65 †	0.92 †	0.68 †
[67]	HOG-DTW	—	—	0.79 †
[85]	Filler-B	0.58 †	—	—
[73]	6-gram CL-Filler	0.61	—	—
[78]	HMM + 2-gram LM	0.72	0.89	0.77
[19]	DTW	0.02	0.37	0.48
	Classic Filler-HMM	0.36	0.83	0.60
	BLSTM	0.78	0.94	0.84
Proposed approach		0.89	0.95	0.91

presented. The formulation of this framework makes it self-evident that KWS is always implicitly or explicitly based on word recognition posterior probabilities and provides probabilistic interpretations to many classical KWS views and methods. Various developments of this framework into specific KWS approaches have been proposed and empirically evaluated. The most efficient and effective of these approaches are based on a word-graph representation of the joint probability distribution of a (line) image region and the text contained in this region. As discussed in previous works, this joint distribution can be advantageously obtained using the same statistical models and training methods, and similar decoding procedures as those used for modern, segmentation-free handwritten text recognition approaches. Therefore, our approaches follow this idea. According to empirical results achieved on several traditional datasets and new, larger corpora, the proposed approaches outperform all the methods proposed and tested so far.

The KWS approaches presented in this paper are all *lexicon-based* (LB). As applied to large-scale indexing, LB methods in general are known to be faster and more accurate than *lexicon-free* (LF) ones, based on raw character processing. However, since LB KWS relies on a predefined lexicon, fixed in the training phase, it does not support queries involving out-of-vocabulary (OOV) keywords. A basic lexicon can be straightforwardly derived from the training transcripts and it can be expanded by including other words expected to appear in the handwritten image collection being considered. These words can be derived from similar texts or glossaries and/or from available vocabularies of the same language and historical period. These issues have not been sufficiently studied in this work. In fact, aiming at obtaining results comparable with other state-of-the-art KWS approaches, the experiments were carried out with query sets extracted from the training texts, thereby guaranteeing that all query words are in-vocabulary. It is worth noting, however, that while the OOV problem may be serious if the indexed vocabulary is small, it becomes much less important with very large vocabularies – which is generally the case in real indexing applications. Several live demonstrators which support this fact can be tested at the Demonstrations page of the TRANSCRIPTORIUM project web site.⁷ These systems also include flexible queries such as searching for word sequences and the BOOLEAN AND/OR/NOT query methods described in [44].

In any case, we are currently developing new approaches for full LF indexing, without having to sacrifice the high effectiveness and efficiency of LB techniques. Two families of methods are being studied.

The first one capitalizes on the very good performance for in-vocabulary keywords of LB methods based on the here proposed probabilistic KWS framework and solves the problem at the query phase, only for OOV words. The idea is to smooth the (implicitly null) relevance probabilities of OOV keywords by relying on the indexed probabilities of “similar” in-vocabulary words. Most of our work in this direction is reviewed or presented in [49]. While reasonably good results are achieved with these methods, they always entail query response time penalties for OOV queries – and these penalties can become prohibitive for large collections of say hundreds of thousands or millions of images.

The other family, also within the here proposed probabilistic KWS framework, abandons the use a lexicon altogether and favors working at the character level. However, it also attempts to keep the good performance of LB indexing by producing relevance probabilities for “words” (actually arbitrary character sequences) which are “discovering” in the very test images (those to be

⁷<http://transcriptorium.eu/demonstrations> → Keyword Indexing & Search

indexed). This kind of work is now in progress, but some of the key ideas have already been published in [72, 73, 6]. Moreover, the large-scale (75 000 page images) indexing task described in [6] has recently been fully accomplished and the resulting real search system can be used from the publicly available HIMANIS project search interface.⁸ The techniques used in this system will be presented in an upcoming publication devoted to probabilistic LF KWS.

9 Acknowledgments

This work has been partially supported through

References

- [1] J. Almazán, A. Gordo, A. Fornés, and E. Valveny. Word spotting and recognition with embedded attributes. *IEEE Transactions on Pattern Analysis and Machine Intelligence*, 36(12):2552–2566, Dec 2014.
- [2] J. Andreu Sánchez, V. Romero, A. H. Toselli, and E. Vidal. ICFHR2014 Competition on Handwritten Text Recognition on Transcriptorium Datasets (HTRtS). In *Frontiers in Handwriting Recognition (ICFHR), 2014 14th International Conference on*, pages 785–790, Sept 2014.
- [3] I. Bazzi, R. Schwartz, and J. Makhoul. An Omnifont Open-Vocabulary OCR System for English and Arabic. *IEEE Trans. on PAMI*, 21(6):495–504, 1999.
- [4] R. Bertolami and H. Bunke. Including language model information in the combination of handwritten text line recognisers. In *Proc. of the International Conference on Frontiers in Handwriting Recognition (ICFHR’08)*, 2008.
- [5] T. Bluche. *Deep Neural Networks for Large Vocabulary Handwritten Text Recognition*. PhD thesis, Université Paris Sud-Paris XI, 2015.
- [6] T. Bluche, S. Hamel, C. Kermorvant, J. Puigcerver, D. Stutzmann, A. H. Toselli, and E. Vidal. Preparatory KWS Experiments for Large-Scale Indexing of a Vast Medieval Manuscript Collection in the HIMANIS Project. In *14th International Conference on Document Analysis and Recognition (ICDAR)*, 2017. Accepted.
- [7] T. Bluche, B. Moysset, and C. Kermorvant. Automatic line segmentation and ground-truth alignment of handwritten documents. In *14th International Conference on Frontiers in Handwriting Recognition (ICFHR’14)*, pages 667–672, Sept 2014.
- [8] T. Causer and V. Wallace. Building a volunteer community: results and findings from Transcribe Bentham. *Digital Humanities Quarterly*, 6(2), 2012.

⁸<http://prhlt-kws.prhlt.upv.es/himanis>

- [9] C. Chelba, J. Silva, and A. Acero. Soft indexing of speech content for search in spoken documents. *Computer Speech & Language*, 21(3):458 – 478, 2007.
- [10] T. K. Chia, K. C. Sim, H. Li, and H. T. Ng. Statistical lattice-based spoken document retrieval. *ACM Trans. Inf. Syst.*, 28(1):2:1–2:30, 2010.
- [11] R. Christiansen and C. Rushforth. Detecting and locating key words in continuous speech using linear predictive coding. *IEEE Trans. on Acoustics, Speech and Signal Processing*, 25(5):361–367, 1977.
- [12] R. O. Duda and P. E. Hart. *Pattern Classification and Scene Analysis*. J. Wiley and Sons, 1973.
- [13] L. Egghe. The measures precision, recall, fallout and miss as a function of the number of retrieved documents and their mutual interrelations. *Information Processing & Management*, 44(2):856–876, 2008.
- [14] S. En, C. Petitjean, S. Nicolas, L. Heutte, and F. Jurie. Region proposal for pattern spotting in historical document images. In *Frontiers in Handwriting Recognition (ICFHR), 2016 15th International Conference on*, pages 367–372. IEEE, 2016.
- [15] S. España-Boquera, M. J. Castro-Bleda, J. Gorbe-Moya, and F. Zamora-Martinez. Improving offline handwritten text recognition with hybrid hmm/ann models. *IEEE Transactions on Pattern Analysis and Machine Intelligence*, 33(4):767–779, April 2011.
- [16] A. Fischer, V. Frinken, H. Bunke, and C. Suen. Improving HMM-based keyword spotting with character language models. In *12th Int. Conference on Document Analysis and Recognition (ICDAR)*, pages 506–510, Aug 2013.
- [17] A. Fischer, A. Keller, V. Frinken, and H. Bunke. Lexicon-free handwritten word spotting using character hmms. *Pattern Recognition Letters*, 33(7):934 – 942, 2012. Special Issue on Awards from ICPR 2010.
- [18] A. Fischer, M. Wuthrich, M. Liwicki, V. Frinken, H. Bunke, G. Viehhauser, and M. Stolz. Automatic transcription of handwritten medieval documents. In *Virtual Systems and Multimedia, 2009. VSMM '09. 15th International Conference on*, pages 137–142, 2009.
- [19] V. Frinken, A. Fischer, R. Manmatha, and H. Bunke. A novel word spotting method based on recurrent neural networks. *Pattern Analysis and Machine Intelligence, IEEE Transactions on*, 34(2):211 –224, feb. 2012.
- [20] A. P. Giotis, G. Sfikas, B. Gatos, and C. Nikou. A survey of document image word spotting techniques. *Pattern Recognition*, 68:310 – 332, 2017.
- [21] A. Graves, S. Fernández, F. Gomez, and J. Schmidhuber. Connectionist Temporal Classification: Labelling Unsegmented Sequence Data with Recurrent Neural Networks. In *Proceedings of the 23rd International Conference on Machine Learning, ICML '06*, pages 369–376, New York, NY, USA, 2006. ACM.

- [22] A. Graves, M. Liwicki, S. Fernández, R. Bertolami, H. Bunke, and J. Schmidhuber. A novel connectionist system for unconstrained handwriting recognition. *IEEE Transactions on Pattern Analysis and Machine Intelligence*, 31(5):855–868, May 2009.
- [23] A. Graves and J. Schmidhuber. Framewise phoneme classification with bidirectional lstm and other neural network architectures. *Neural Networks*, 18(5):602 – 610, 2005. IJCNN 2005.
- [24] A. Hast and A. Fornés. A segmentation-free handwritten word spotting approach by relaxed feature matching. In *Document Analysis Systems (DAS), 2016 12th IAPR Workshop on*, pages 150–155. IEEE, 2016.
- [25] M. P. i Gadea, A. H. Toselli, and E. Vidal. Projection profile based algorithm for slant removal. In *Proceedings of ICIAR*, 2004.
- [26] F. Jelinek. *Statistical Methods for Speech Recognition*. MIT Press, 1998.
- [27] E. Kavallieratou and E. Stamatatos. Improving the quality of degraded document images. In *Document Image Analysis for Libraries, 2006. DIAL '06. Second International Conference on*, pages 10 pp. –349, april 2006.
- [28] M. Khayyat, L. Lam, and C. Y. Suen. Learning-based word spotting system for arabic handwritten documents. *Pattern Recognition*, 47(3):1021–1030, 2014.
- [29] R. Kneser and H. Ney. Improved backing-off for N-gram language modeling. In *International Conference on Acoustics, Speech and Signal Processing (ICASSP '95)*, volume 1, pages 181–184, Los Alamitos, CA, USA, 1995.
- [30] A. Kolcz, J. Alspector, M. Augusteijn, R. Carlson, and G. Viorel Popescu. A Line-Oriented Approach to Word Spotting in Handwritten Documents. *Pattern Analysis & Applications*, 3:153–168, 2000.
- [31] M. Kozielski, J. Forster, and H. Ney. Moment-based image normalization for handwritten text recognition. In *Proceedings of the 2012 International Conference on Frontiers in Handwriting Recognition, ICFHR '12*, pages 256–261, Washington, DC, USA, 2012. IEEE Computer Society.
- [32] G. Kumar and V. Govindaraju. A bayesian approach to script independent multilingual keyword spotting. In *14th International Conference on Frontiers in Handwriting Recognition (ICFHR)*, pages 357–362. IEEE, 2014.
- [33] M. R. Kumar, R. Pradeep, P. Babu, and B. P. Kumar. A simple text-line segmentation method for handwritten documents. *IJCA Proceedings on National Conferecne on Advanced Computing and Communications 2012*, (1):46–61, 2012.
- [34] V. Lavrenko, T. M. Rath, and R. Manmatha. Holistic word recognition for handwritten historical documents. In *Document Image Analysis for Libraries, 2004. Proceedings. First International Workshop on*, pages 278–287, 2004.

- [35] Y. LeCun, B. E. Boser, J. S. Denker, D. Henderson, R. E. Howard, W. E. Hubbard, and L. D. Jackel. Handwritten digit recognition with a back-propagation network. In *Advances in neural information processing systems*, pages 396–404, 1990.
- [36] Y. Li, Y. Zheng, D. Doermann, and S. Jaeger. Script-independent text line segmentation in freestyle handwritten documents. *IEEE Trans. on PAMI*, 30(8):1313–1329, 2008.
- [37] L. Likforman-Sulem, A. Zahour, and B. Taconet. Text line segmentation of historical documents: a survey. *Int. J. Doc. Anal. Recognit.*, 9:123–138, April 2007.
- [38] G. Louloudis, B. Gatos, I. Pratikakis, and C. Halatsis. Text line and word segmentation of handwritten documents. *Pattern Recognition*, 42(12):3169–3183, 2009.
- [39] A. L. Maas, A. Y. Hannun, and A. Y. Ng. Rectifier nonlinearities improve neural network acoustic models. In *Proc. ICML*, volume 30, 2013.
- [40] C. D. Manning, P. Raghavan, and H. Schtze. *Introduction to Information Retrieval*. Cambridge University Press, New York, NY, USA, 2008.
- [41] U.-V. Marti and H. Bunke. Using a Statistical Language Model to Improve the Performance of an HMM-Based Cursive Handwriting Recognition System. *Int. Journal of Pattern Recognition and Artificial Intelligence*, 15:65–90, 2001.
- [42] U.-V. Marti and H. Bunke. The iam-database: an english sentence database for offline handwriting recognition. *International Journal on Document Analysis and Recognition*, 5:39–46, 2002.
- [43] A. Niculescu-Mizil and R. Caruana. Predicting good probabilities with supervised learning. In *Proceedings of the 22nd international conference on Machine learning*, pages 625–632. ACM, 2005.
- [44] E. Noya-García, A. H. Toselli, and E. Vidal. *Simple and Effective Multi-word Query Spotting in Handwritten Text Images*, pages 76–84. Springer International Publishing, Cham, 2017.
- [45] S. Ortmanns, H. Ney, and X. Aubert. A Word Graph Algorithm for Large Vocabulary Continuous Speech Recognition. *Computer Speech and Language*, 11(1):43–72, Jan. 1997.
- [46] D. Povey, A. Ghoshal, G. Boulianne, L. Burget, O. Glembek, N. Goel, M. Hannemann, P. Motlicek, Y. Qian, P. Schwarz, J. Silovsky, G. Stemmer, and K. Vesely. The Kaldi Speech Recognition Toolkit. In *IEEE 2011 Workshop on Automatic Speech Recognition and Understanding*. IEEE Signal Processing Society, 2011.
- [47] D. Povey, M. Hannemann, G. Boulianne, L. Burget, A. Ghoshal, M. Janda, M. Karafiát, S. Kombrink, P. Motlíček, Y. Qian, et al. Generating exact lattices in the WFST framework. In *Acoustics, Speech and Signal Processing (ICASSP), 2012 IEEE International Conference on*, pages 4213–4216. IEEE, 2012.
- [48] J. Puigcerver. Are multidimensional recurrent layers really necessary for Handwritten Text Recognition? In *2017 14th International Conference on Document Analysis and Recognition (ICDAR)*, 2017. Accepted.

- [49] J. Puigcerver, A. H. Toselli, and E. Vidal. Querying out-of-vocabulary words in lexicon-based keyword spotting. *Neural Computing and Applications*, 28(9):2373–2382, Sep 2017.
- [50] S. Ren, K. He, R. Girshick, and J. Sun. Faster R-CNN: Towards real-time object detection with region proposal networks. *IEEE transactions on pattern analysis and machine intelligence*, 39(6):1137–1149, 2017.
- [51] S. B. Rezaei, A. Sarrafzadeh, and J. Shanbehzadeh. Skew detection of scanned document images. In *International MultiConference of Engineers and Computer Scientists (IMECS)*, volume 1, Hong Kong, Mar. 2013.
- [52] S. Robertson. A new interpretation of average precision. In *Proc. of the International ACM SIGIR conference on Research and development in information retrieval (SIGIR '08)*, pages 689–690, New York, NY, USA, 2008. ACM.
- [53] J. A. Rodríguez and F. Perronnin. Local gradient histogram features for word spotting in unconstrained handwritten documents. In *ICFHR 2008 (Int. Conf. on Frontiers in Handwriting Recognition)*, pages 7–12, 2008.
- [54] J. A. Rodríguez-Serrano and F. Perronnin. Handwritten word-spotting using hidden markov models and universal vocabularies. *Pattern Recogn.*, 42:2106–2116, September 2009.
- [55] J. A. Rodríguez-Serrano and F. Perronnin. Handwritten word-spotting using hidden Markov models and universal vocabularies. *Pattern Recognition*, 42:2106–2116, September 2009.
- [56] V. Romero, M. Pastor, A. H. Toselli, and E. Vidal. Criteria for handwritten off-line text size normalization. In *Procc. of the IASTED Int. Conf. on Visualization, Imaging, and Image Processing (VIIP 06)*, Palma de Mallorca, Spain, August 2006. 6 pages.
- [57] V. Romero, A. H. Toselli, and E. Vidal. *Multimodal Interactive Handwritten Text Transcription*. Series in Machine Perception and Artificial Intelligence (MPAI). World Scientific Publishing, 2012.
- [58] R. Rose and D. Paul. A Hidden Markov Model based keyword recognition system. In *Int. Conference on Acoustics, Speech, and Signal Processing (ICASSP '90)*, pages 129–132 vol.1, apr 1990.
- [59] J. A. Sánchez, V. Romero, A. H. Toselli, and E. Vidal. ICFHR2016 Competition on Handwritten Text Recognition on the READ Dataset. In *15th International Conference on Frontiers in Handwriting Recognition (ICFHR'16)*, pages 630–635, Oct 2016.
- [60] A. Sanchis, A. Juan, and E. Vidal. A word-based naive bayes classifier for confidence estimation in speech recognition. *Audio, Speech, and Language Processing, IEEE Transactions on*, 20(2):565–574, Feb 2012.
- [61] J. Sauvola and M. Pietikäinen. Adaptive document image binarization. *Pattern Recognition*, 33:225–236, 2000.

- [62] M. Schuster and K. K. Paliwal. Bidirectional recurrent neural networks. *IEEE Transactions on Signal Processing*, 45(11):2673–2681, Nov 1997.
- [63] M. Stauffer, A. Fischer, and K. Riesen. Speeding-up graph-based keyword spotting in historical handwritten documents. In V. M. Foggia P., Liu CL., editor, *Graph-Based Representations in Pattern Recognition (GbrPR)*, volume 10310 of *Lecture Notes in Computer Science*. Springer, 2017.
- [64] I. Szőke, P. Schwarz, L. Burget, M. Karafiát, and J. Cernocký. Phoneme based acoustics keyword spotting in informal continuous speech. In *Radioelektronika 2005*, pages 195–198. Faculty of Electrical Engineering and Communication BUT, 2005.
- [65] L. Tarazón, D. Pérez, N. Serrano, V. Alabau, O. Ramos Terrades, A. Sanchis, and A. Juan. Confidence Measures for Error Correction in Interactive Transcription Handwritten Text. In *Image Analysis and Processing (ICIAP '09)*, volume 5716 of *Lecture Notes in Computer Science*, pages 567–574. Springer Berlin / Heidelberg, 2009.
- [66] K. Terasawa and Y. Tanak. Slit style hog feature for document image word spotting. In *Document Analysis and Recognition, 2009. ICDAR '09. 10th International Conference on*, pages 116–120, July 2009.
- [67] K. Terasawa and Y. Tanaka. Slit style hog feature for document image word spotting. In *2009 10th International Conference on Document Analysis and Recognition*, pages 116–120, July 2009.
- [68] S. Thomas, C. Chatelain, L. Heutte, and T. Paquet. Alpha-Numerical Sequences Extraction in Handwritten Documents. In *Proc. of the Int. Conference on Frontiers in Handwriting Recognition (ICFHR '10)*, pages 232–237, Washington, DC, USA, 2010. IEEE Computer Society.
- [69] T. Tieleman and G. Hinton. Lecture 6.5-rmsprop: Divide the gradient by a running average of its recent magnitude. *COURSERA: Neural networks for machine learning*, 4(2), 2012.
- [70] A. H. Toselli, A. Juan, D. Keysers, J. González, I. Salvador, H. Ney, E. Vidal, and F. Casacuberta. Integrated Handwriting Recognition and Interpretation using Finite-State Models. *Int. Journal of Pattern Recognition and Artificial Intelligence*, 18(4):519–539, June 2004.
- [71] A. H. Toselli, L. A. Leiva, I. Bordes-Cabrera, C. Hernández-Tornero, B. Vicent, and E. Vidal. Transcribing a 17th century botanical manuscript: Longitudinal interactive transcription evaluation and ground truth production. *Digital scholarship in the humanities*, 2017.
- [72] A. H. Toselli, J. Puigcerver, and E. Vidal. Context-aware lattice based filler approach for key word spotting in handwritten documents. In *Document Analysis and Recognition (ICDAR), 2015 13th International Conference on*, pages 736–740, Aug 2015.
- [73] A. H. Toselli, J. Puigcerver, and E. Vidal. Two methods to improve confidence scores for lexicon-free word spotting in handwritten text. In *Frontiers in Handwriting Recognition (ICFHR'16), 2016 15th International Conference on*, pages 349–354. IEEE, 2016.

- [74] A. H. Toselli, V. Romero, M. P. i Gadea, and E. Vidal. Multimodal interactive transcription of text images. *Pattern Recognition*, 43(5):1814–1825, 2010.
- [75] A. H. Toselli, V. Romero, and E. Vidal. Word graphs size impact on the performance of handwriting document applications. *Neural Computing and Applications*, 28(9):2477–2487, Sep 2017 (first online 2016).
- [76] A. H. Toselli and E. Vidal. Fast HMM-Filler approach for Key Word Spotting in Handwritten Documents. In *Proc. of the 12th Int. Conference on Document Analysis and Recognition (ICDAR '13)*, Washington, DC, USA, 2013. IEEE Computer Society.
- [77] A. H. Toselli and E. Vidal. Handwritten Text Recognition Results on the Bentham Collection with Improved Classical N-Gram-HMM Methods, booktitle = Proceedings of the 3rd International Workshop on Historical Document Imaging and Processing. HIP '15, pages 15–22, New York, NY, USA, 2015. ACM.
- [78] A. H. Toselli, E. Vidal, V. Romero, and V. Frinken. HMM word graph based keyword spotting in handwritten document images. *Information Sciences*, 370-371:497 – 518, 2016.
- [79] H. Ventsel. *Théorie des Probabilités*. Éditions MIR. Moscou, 1973.
- [80] E. Vidal, A. H. Toselli, and J. Puigcerver. High performance query-by-example keyword spotting using query-by-string techniques. In *2015 13th International Conference on Document Analysis and Recognition (ICDAR)*, pages 741–745, Aug 2015.
- [81] A. Vinciarelli, S. Bengio, and H. Bunke. Offline Recognition of Unconstrained Handwritten Texts Using HMMs and Statistical Language Models. *IEEE Transactions on Pattern Analysis and Machine Intelligence*, 26(6):709–720, June 2004.
- [82] B. Wicht, A. Fischer, and J. Hennebert. Deep learning features for handwritten keyword spotting. In *2016 23rd International Conference on Pattern Recognition (ICPR)*, pages 3434–3439, Dec 2016.
- [83] B. Wicht, A. Fischer, and J. Hennebert. Keyword spotting with convolutional deep belief networks and dynamic time warping. In *Proc. 25th Int. Conf. on Artificial Neural Networks*, page 113–120, 2016.
- [84] S. Wshah, G. Kumar, and V. Govindaraju. Script Independent Word Spotting in Offline Handwritten Documents Based on Hidden Markov Models. In *Frontiers in Handwriting Recognition (ICFHR), 2012 International Conference on*, pages 14–19, Sept 2012.
- [85] S. Wshah, G. Kumar, and V. Govindaraju. Statistical script independent word spotting in offline handwritten documents. *Pattern Recognition*, 47(3):1039–1050, 2014.
- [86] S. Young, J. Odell, D. Ollason, V. Valtchev, and P. Woodland. *The HTK Book: Hidden Markov Models Toolkit V2.1*. Cambridge Research Laboratory Ltd, Mar. 1997.
- [87] R. Zens and H. Ney. Word graphs for statistical machine translation. In *Proceedings of the ACL Workshop on Building and Using Parallel Texts, ParaText '05*, pages 191–198, Stroudsburg, PA, USA, 2005. Association for Computational Linguistics.

- [88] M. Zhu. Recall, Precision and Average Precision. Working Paper 2004-09 Department of Statistics & Actuarial Science - University of Waterloo, August 26 2004.